

APWR-0452-NP

Non-Proprietary Version

AP600  
VORTEX MITIGATOR DEVELOPMENT TEST  
FOR  
RCS MID-LOOP OPERATION

BY  
L. K. LAU  
T. S. ANDREYCHEK

SEPTEMBER 1988

APPROVED:

*Theo van de Venne*

T. van de Venne, Engineering Manager  
Advanced PWR Development

Work Performed Under Shop Order ALWP 27K00

8051a.1d/101288

9407180246 940706  
PDR ADOCK 05200003  
A PDR

APWR-0452-NP

Non-Proprietary Version

AP600  
VORTEX MITIGATOR DEVELOPMENT TEST  
FOR  
RCS MID-LOOP OPERATION

BY  
L. K. LAU  
T. S. ANDREYCHEK

SEPTEMBER 1988

APPROVED: *T. van de Venne*

T. van de Venne, Engineering Manager  
Advanced PWR Development

Work Performed Under Shop Order ALWP 27K00

## TABLE OF CONTENTS

<u>SECTION</u>	<u>TITLE</u>	<u>PAGE</u>
1.0	ABSTRACT	
2.0	BACKGROUND INFORMATION AND INTRODUCTION	
	2.1 BACKGROUND INFORMATION	
	2.2 INTRODUCTION	
3.0	SUMMARY AND RECOMMENDATION	
4.0	TEST PROGRAM	
	4.1 TEST PURPOSE AND OBJECTIVES	
	4.2 TEST MODEL DESCRIPTION	
	4.3 TEST MODEL INSTRUMENTATION	
	4.4 TEST MODELING TECHNIQUE	
5.0	DESCRIPTION OF TEST OPERATIONS	
6.0	DISCUSSION OF TEST RESULTS AND SUMMARY	
7.0	BIBLIOGRAPHY	
8.0	APPENDIX	
	APPENDIX A - SAMPLE CALCULATIONS	
	APPENDIX B - VOID METER DESCRIPTION/CALIBRATION	

## LIST OF ILLUSTRATIONS

<u>FIGURE NUMBER</u>	<u>TITLE</u>	<u>PAGE</u>
4.1-1	Simulated RHR Installed with Cruciform	
4.1-2	Simulated RHR Pipe with Step Nozzle	
4.2-1	Test Model General Assembly (2 Sheets)	
4.2-2	Test System Flow Diagram	
6.1	Vortexing Water Level vs. Froude Number	
6.2	Comparison of Test Results	
6.3	Comparison of Test Results	
6.4	Comparison of Test Results	
6.5	Comparison of Test Results	
6.6	Comparison of Test Results - 3" Intermediate Pipe vs. Simulated RHR Pipe	
6.7	Air Entrainment vs. Water Level	
6.8	Vortexing Water Level vs. Froude Number	
6.9	Comparison of Test Results	
6.10	Vortexing Water Level vs Froude Number	
6.11	Comparison of Test Results	
6.12	Vortexing Water Level vs. Froude Number	
6.13	Comparison of Test Results	
6.14	Comparison of Test Results	
6.15	Comparison With MHI Test	
6.16	Vortexing Water Level vs. Froude Number	
6.17	Comparison of Data With Different Simulated RHR Pipe	

LIST OF TABLES

<u>TABLE NUMBER</u>	<u>TITLE</u>	<u>PAGE</u>
4.1	Equipment Parameter Summary	
6.1	Summary of Test And Predicted Plant Results (3 Sheets)	

## 1.0 ABSTRACT

Mid-loop operation refers to nuclear plant operation for which the water level in the reactor is dropped to approximately mid-height of the hot leg as it exits the reactor vessel while the residual heat removal (RHR) pump is operating at a pre-selected flow rate. Such an operation would occur during refueling operations. A comprehensive test program was performed to investigate the potential vortex behavior at the RHR line/hot leg junction of the AP600 plant during mid-loop operation. In particular, the ingestion of air by the vortex and the resulting influence on the overall RHR system performance during mid-loop operation were studied in detail.

Different RHR nozzle geometries for the AP600 plant were studied parametrically to assess the influence of geometry on vortex formation and resulting void ingestion. The optimal hot leg/RHR nozzle design combination for implementation in the AP600 plant was defined as that which minimized ingestion of voids into the RHR flow during mid-loop operation.

The test results show that an intermediate step nozzle, strategically located between the hot leg and the traditional RHR nozzle, can reduce the momentum of the vortex effectively and eventually results in the breakup of the vortex at a water level much lower than the mid-loop level of the hot leg.

Based on the test results, a unique hot leg-intermediate step nozzle-RHR nozzle arrangement is recommended for AP600. The hot leg of the AP600 has a 31 inch inside diameter. The recommended step nozzle has an inside diameter of at least [ ]<sup>a,b</sup> inches and a length of at least [ ]<sup>a,b</sup> inches. By comparison, the present RHR nozzle has an inside diameter of [ ]<sup>a,b</sup> inches. The recommended step nozzle is located between the bottom of the hot leg and the top of the RHR nozzle.

## 2.0 BACKGROUND INFORMATION AND INTRODUCTION

### 2.1 Background Information

There have been over 140 incidents reported to the NRC since 1977 concerning the loss of Residual Heat Removal System (RHRS) operation due to human errors, equipment malfunctions and loss of fluid inventory in the reactor coolant system. Among the incidents reported, it has been determined that 37 of them occurred because the fluid level in the reactor coolant system was drained sufficiently low as to adversely affect RHR pump operation. When the RCS water level is drained below a certain level, a vortex begins to form and the RHR pumps are cavitated or become airborne. Once airborne, the RHR pumps must be manually stopped to prevent damage. In current PWR plants RHR pumps are also used as safety injection pumps. Consequently, with the RHR pumps stopped, both decay heat removal and low head safety injection functions are lost, allowing for a possible heatup of the RCS inventory that may result core uncover. An extended period of core uncover may cause fuel damage.

The time margin available for restoring the RHRS, or establishing alternate methods of heat removal (prior to bulk boiling, core uncover, fuel damage, etc.) depends on the initial RCS temperature, the decay heat rate (which is dependent on time interval elapsed from reactor trip to RHRS failure and core power operation history), and the initial RCS inventory.

One worst case scenario would be the loss of RHRS during mid-loop operation. Mid-loop operation is an operation where the RCS coolant inventory is drained to approximately the mid-level of the hot leg to perform steam generator inspections or repairs. The RHR pump operates at its designated flow rate with the reduced RCS inventory. If the RCS inventory drops below a certain level (which may occur rapidly since there is little level margin in the RCS), a vortex begins to form, air is injected into the RHR flow, and the RHR pump cavitates, resulting in the loss of RHRS operation. The reduced RCS inventory minimizes the time available to recover the RHRS prior to bulk boiling and core uncover.

Both NRC AEOD (Office for Analysis and Evaluation of Operational Data) and licensees analyzed the loss of RHRS during mid-loop operation. The conclusion drawn from the analysis is that core uncovering could result on the order of one to three hours after loss of RHRS operation, unless timely corrective actions are taken.

On August 18, 1983, Sequoyah-2 nuclear power plant reported a loss of RHRS event to the NRC. It had a 92 degrees F. heatup in 77 minutes with reduced RCS inventory.

Recently, on April 10, 1987 the Diablo Canyon unit 2 reactor experienced a loss of RHRS during the mid-loop operation with reduced RCS inventory. The RHRS was inoperative for 85 minutes. During this time period the RCS temperature increased from 87 degrees F to bulk boiling and a moderate repressurization occurred.

Due to both the high number of events reported, the perception of a lack of improvement with regard to RHRS operation at reduced RCS inventory levels since 1977 despite several NRC Inspection and Enforcement (I&E) Notices, the issuance of an AEOD report and an NSAC report both addressing problems with mid-loop operation, NRC has become very concerned and believes that a stronger approach to addressing the loss of RHRS is required. Consequently, a 10CFR50.54(f) letter was issued on July 1 1987 to all PWRs and holders of construction permits for PWR's to address the potential loss of RHRS problem

## 2.2 Introduction

AP600 differs from the traditional PWR design in that it does not have an independent RHR system. The traditional decay heat removal function is combined with the spent fuel cooling function to form a Spent Fuel Cooling System (SFCS). The two identical pump and heat exchanger trains can be used interchangeably, thereby satisfying the redundant capacity requirement placed on the RHRS. It should be noted that because of the passive nature of the AP600 Safety Systems the RHR pumps are no longer safety injection pumps.



However, the loss of RHR cooling concerns associated with mid-loop operation in the current plants are still applicable to AP600 SFCS. In the AP600 design, the steam generator inspection and repairs require that the hot leg water level be drained to a near mid-loop level. The decay heat removal pump takes suction from the hot leg while the mid-loop operation is in progress. Too low a hot leg level may induce a vortex which could ingest air into the RHR flow, causing the pump to cavitate and resulting in similar consequences as for a traditional PWR plant.

The current experimental program dealt with the vortex generation problem during mid-loop operation for the AP600 design. The vortex phenomenon was studied in detail using a scaled, clear plastic model with the hot leg, the reactor vessel and the RHR line properly modeled. A number of designs thought to possibly break up vortices (called vortex breakers) were tested to investigate their influence on both the water level in the hot leg at which a vortex would form and the strength of the vortex that would form. A recommended vortex breaker design was selected from the test results.

### 3.0 SUMMARY AND RECOMMENDATION

#### 3.1 GENERAL SUMMARY

This section summarizes the test data from the current test program. Comparison of the data collected from the current program to data from other tests performed in the industry is given in Section 6.0.

- (a) At a given RHR flow rate there exists a critical water level in the hot leg below which the vortex will cause air to be entrained in the water flowing to the pump. This critical water level is called the critical vortexing water level.
- (b) Two major parameters affects the critical vortexing water level; the circulation in the flow approaching an intake, and the Froude number. The circulation effect is very much geometry dependent. The Froude number is very much flow velocity dependent. For a given geometry the Froude number plays a major role in determining the critical vortexing water level. Higher Froude number results with a higher critical vortexing level. Consequently, low flow rate is recommended during the mid-loop operation.
- (c) When the critical vortexing water level is plotted against the Froude number on a log-log scale, the result is two straight lines. These two straight lines of different slopes meet at a knee point (See Figures 6.1, 6.16 and 6.17 for examples). This knee point is very important in that Froude numbers greater than 1.0 result in the air contained in the vortex flowing along with the water rapidly, and consequently cavitating the pump. When the Froude number is slightly below the knee point, a very small amount of air flows along with the water to the pump. As the Froude number is further reduced below the knee point, no air travels along with the water to the pump at all.

(d) Comparison of test results shows that the step nozzle configuration has the lowest critical vortexing water level, lower than both the bottom mounted and the 45 degree mounted RHR nozzle configurations. Moreover, with the step nozzle configuration, the pump and system operation is still steady even when the water level in the hot leg drops below the critical vortexing water level. See section 6.3 for more details.

(e) Step nozzles having the following geometric parameter ranges were tested:

- i) The ratio between the step nozzle ID and the hot leg ID is greater than or equal to  $\left[ \quad \right]^{a,b}$
- ii) The ratio between the step nozzle ID and the RHR nozzle ID is greater than or equal to  $\left[ \quad \right]^{a,b}$
- iii) The ratio between the length and the ID of the step nozzle is greater than or equal to approximately  $\left[ \quad \right]^{a,b}$

Over the range of geometric parameters tested, the data collected provides the following prediction for critical vortexing water level:

$$h/d = \left[ \quad \right]^{a,b}$$

where

h = the critical vortexing water level with respect to the bottom of the hot leg ID.

d = inside diameter of the step nozzle

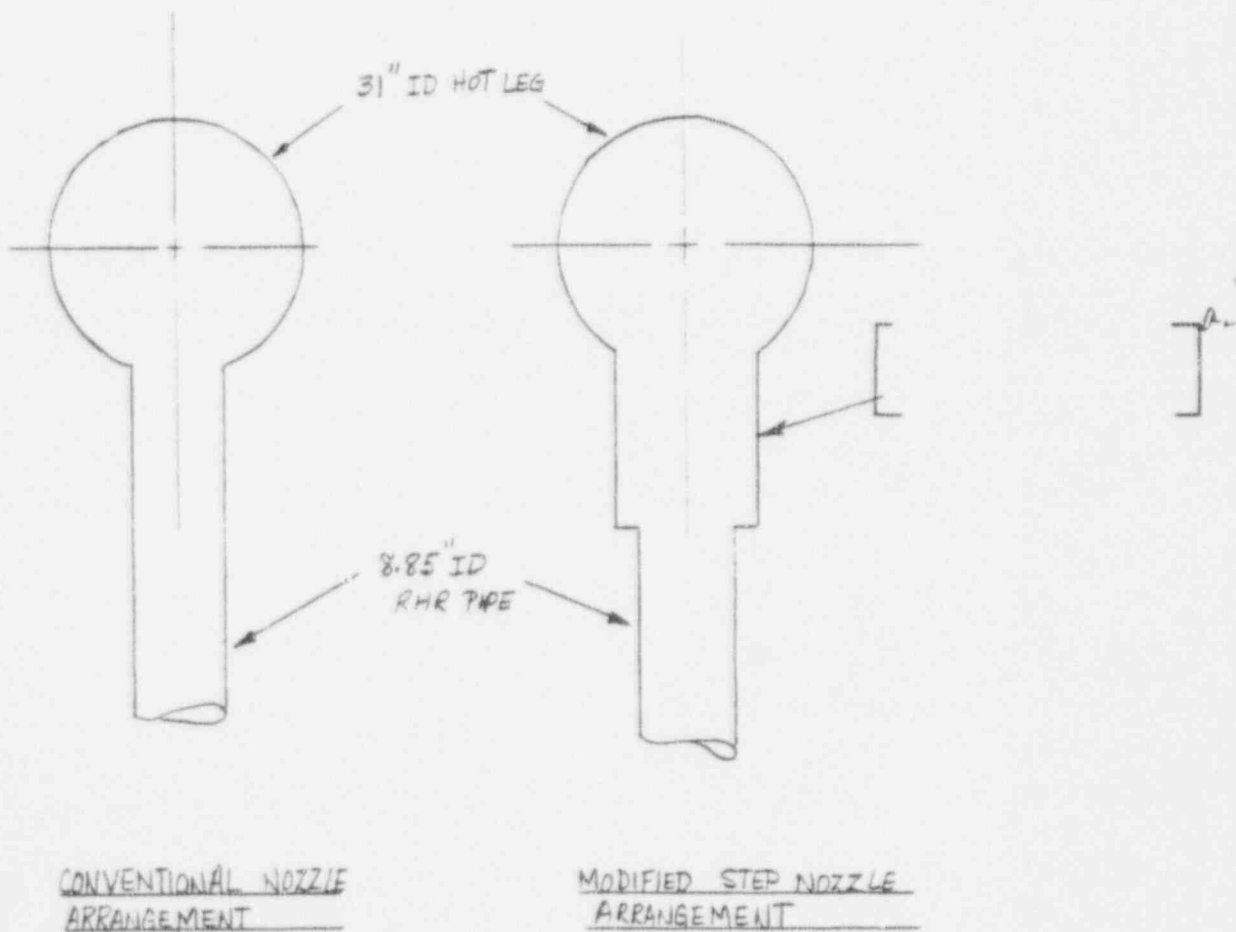
Fr = Froude number.

For the AP600 plant with a step nozzle between the hot leg and RHR line, the critical vortexing water level in the hot leg at 2000 gpm flow rate is predicted to be 10.42 inches above the hot leg bottom. This water level is significantly lower than the mid-loop level of 15.5 inches.

### 3.2 RECOMMENDATION

Based on the data collected, it is concluded that the step nozzle configuration is the most desirable design for implementation in the AP600. The most optimal configuration was found to be arrangement 3 of section 6.3, i.e., a step nozzle [ ]<sup>a, b</sup> connected to the bottom of the hot leg with the RHR pipe connected to its bottom.

Both the conventional present nozzle arrangement and the modified step nozzle configuration are shown below.



## 4.0 TEST PROGRAM

### 4.1 TEST PURPOSE AND OBJECTIVES

The following test objectives are identified:

- (a) Measure the critical vortexing water level at different pump flow rates. The critical vortexing water level is defined as that water level in the simulated hot leg below which air would be drawn through the simulated RHR pipe and into the pump suction.
- (b) Measure the critical vortexing water level at different pump flow rates, with a cruciform installed in the simulated RHR pipe, as shown in figure 4.1-1
- (c) Measure the critical vortexing water level at different pump flow rates, with step nozzles of different size and length installed, as shown in figure 4.1-2
- (d) Measure and record the percentage of air drawn through the simulated RHR pipe (and into the pump) when the hot leg water level drops below the critical vortexing water level, for all three cases above.

### 4.2 TEST MODEL DESCRIPTION

Figure 4.2-1 shows the general assembly of the test model. It uses a simulated hot leg, a simulated RHR pipe connected to the bottom of the hot leg, and a simulated reactor vessel. The test model is constructed of plastic materials for visual inspection of the vortex formation. The instrumentation used to measure the percentage of the air entrained in the liquid also requires that the test model be made of electrically non-conductive materials. Consequently, clear acrylic is used to fabricate the test article.

The linear scale used is 0.226. This linear scale makes the inside diameter of the simulated hot leg to be 7.0 inches, and the inside diameter of the

simulated RHR pipe to be 2.0 inches. The following table compares the dimensions of both the AP600 plant components and the test model components.

COMPONENTS	TEST MODEL	AP600
HOT LEG INSIDE DIA.	7.0 INCHES	31.0 INCHES
RHR PIPE INSIDE DIA.	2.0 INCHES	8.85 INCHES
FIRST STEP NOZZLE ID.	[ ] <sup>a,b</sup> INCHES	[ ] <sup>a,b</sup> INCHES
SECOND STEP NOZZLE ID.	[ ] INCHES	[ ] INCHES

Additionally, the interface geometry between the reactor vessel, the hot leg and the RHR line in the plant is properly modeled in the test. This similarity in geometry is of utmost importance in applying the test results to the plant.

The simulated reactor vessel is basically a large tank (71"x24"x48") with a water volume of approximately 354 gallons. Its sole function is to supply water to the simulated hot leg and to receive water from the pump. It is constructed with polypropylene sheets and is laterally supported with wooden frames. The tank internals consists of two baffle plates, a suction nozzle, a discharge piping, a main drain connection and connections for instrumentation calibration.

The (two) plastic baffle plates inserted inside the tank are arranged to minimize or prevent any potential wave motion transmitted to the simulated hot leg. The return line from the pump discharge to the tank is also located on the far end from the simulated hot leg. All these arrangements are made to ensure steady flow to the hot leg.

Connected to the upper end of the tank is the simulated hot leg. The hot leg inside diameter for the AP600 plant is currently set at 31 inches. The simulated hot leg inside diameter is 7.0 inches. Consequently, the linear scale is 0.226. The other end of the simulated hot leg is curved up to simulate the steam generator connection. However, no steam generator is modeled in the test, and this curved end is capped. The length of the

simulated hot leg is approximately 76 inches. It should be pointed out that this length of 76 inches is not a scaled length; it is approximately 33 inches longer than a properly scaled hot leg. This longer length should have no effective influence on the vortex formation. The suction nozzle between the tank (the simulated reactor vessel) and the simulated hot leg is shaped to model, as close as practical, the Reactor Vessel hot leg nozzle configuration. This smooth nozzle shape and chamfered edges reduce entrance turbulence.

The simulated RHR pipe is connected to the bottom of the hot leg. This arrangement models the geometry in the plant. The inside diameter of the RHR line in the plant is 8.75 inches (10" sch.140 ) resulting in a scaled RHR line of approximately 2.0 inches. Installed inside the bottom end of the simulated RHR line is a void meter which measures the percentage of air passing through.

The simulated RHR line connects to the suction of the pump. The discharge line of the pump returns to the tank. There is a flow meter installed at the discharge of the pump to measure the pump flow rate.

The pump is a Grainger-Teel self priming 2 H.P. No. IP897 centrifugal type with a design point of 103 gpm at 30 Ft head. The pump is driven by 230 VAC single phase power supply.

A number of valves are used for flow control, isolation and drain functions.

Figure 4.2-2 is a flow diagram of the test hydraulic loop. Table 4-1 summarizes the equipments used for this test program.

The test studied the vortex phenomenon using different interface relationships between the hot leg and the simulated RHR line as follows:

- (a) 2.0" ID pipe connected to the bottom of the simulated hot leg.
- (b) 2.0" ID pipe connected to the bottom of the simulated hot leg, and a cruciform installed inside the top end of the simulated RHR line as

shown in figure 4.1-1. The cruciform is 0.125 inches in thickness and 4.0 inches in length.

- (c) An intermediate pipe (step nozzle) of [ ]<sup>a,b</sup> inch inside diameter and 12 inches in length is connected to the bottom end of the simulated hot leg. The 2.0 inch ID simulated RHR pipe is connected to the bottom end of the step nozzle, as shown in figure 4.1-2
- (d) Same as c. with a step nozzle of [ ]<sup>a,b</sup> inch ID and a length of 12 inches.
- (e) Same as c. with a step nozzle of [ ]<sup>a,b</sup> inch ID and a length of 5.56 inches.
- (f) Same as c. with a step nozzle of [ ]<sup>a,b</sup> inch ID and a length of 2.875 inches.
- (g) Same as c. with a step nozzle of [ ]<sup>a,b</sup> inch ID and a length of 4.3 inches.

### 4.3 TEST MODEL INSTRUMENTATION

#### 4.3.1 Flow

Flow during the test was monitored by 2 flow gauges in each of the parallel paths (as identified as FI-1 and FI-2 in figure 4.2-2) downstream of the pump.

The gauges were direct reading flow orifices from RCM Industries, made of plastic material. The parameters are as follows:

FI-1. 2" - 15 to 100 gpm range, No. 9858K55

FI-2. 1" - 3 to 20 gpm range, No. 9858K53



#### 4.3.2 Pressure

Three pressure gauges were used to monitor the pump inlet and outlet conditions.

The parameters are as follows:

PI-1 and PI-2: these suction gauges had a 0 to 30" Hg (absolute) and a 0 to 5 psig range, respectively.

PI-3: this discharge gauge had a 0 to 60 psig range

#### 4.3.3 Level Measurement

Level measurement readings were taken at the following system locations:

- o L-1: holdup tank level
- o L-2: entrance level to main loop pipe
- o L-3: upstream of the simulated RHR suction nozzle
- o L-4: downstream of the simulated RHR suction nozzle
- o L-5: downstream of void meter

Tygon hose of 1/2" diameter was routed from the measurement point to the readout location on the end of the main loop piping.

#### 4.3.4 Void Fraction Meter

A description of the void meter is given in Appendix B.

### 4.4 TEST MODELING TECHNIQUE

#### 4.4.1 Background

A literature search was conducted prior to the design of the test model. Almost all material studied the vortexing phenomenon with the intake pipe

connected to the bottom of the reservoir. Vortexing phenomenon was studied experimentally and analytically, with the following parameters being identified as important to understanding the vortex phenomena:

- (a) Froude Number (Fr): The Froude number is the ratio of dynamic force to weight. Mathematically, it can be expressed as

$$Fr = \frac{v}{(gd)^{0.5}}$$

where

- Fr = Froude number, dimensionless
- v = fluid velocity at the intake pipe
- g = gravitational acceleration
- d = inside diameter of the intake pipe

- (b) Viscosity Parameter (Nv): The viscosity parameter is the ratio of the Reynolds number and the Froude number. Mathematically, it can be expressed as

$$Nv = Re/Fr$$

$$= \frac{g^{1/2} d^{3/2}}{v}$$

where

- Re = Reynolds number
- v = kinematic viscosity
- g, d are as defined previously.

- (c) Weber Number (We): The Weber number is the ratio of the inertia force to the surface tension force. Mathematically, it can be expressed as

$$We = \frac{\rho v^2 d}{\sigma}$$

where

$\rho$  = fluid density

$\sigma$  = surface tension

The Weber number models the effect of surface tension on vortex formation.

- (d) Relative Submergence ( $h/d$ ): The relative submergence is the ratio of the submergence depth to the intake pipe inside diameter.

Vortex formation is a sensitive and complicated phenomenon. It is highly dependent on the circulation of the fluid, the flow rate, the water level at the reservoir, and the intake pipe diameter. The above four major parameters can be arranged with  $h/d$  as a function of the other three parameters, and their relationship can be found experimentally. Reference 2 investigated vortex formation phenomenon with a bottom mounted intake pipe of various sizes and a setup that could effectively control the circulation of the fluid. The experiments revealed the following findings:

- (a) There is no influence of surface tension on the critical vortexing water level when the Weber number is greater than or equal to 120. The critical vortexing water level is defined as the water level at the reservoir below which vortex would be drawn through the intake pipe.
- (b) The critical vortexing water level generally decreases with increase in viscosity of the fluid due to reduction in the strength of circulation with increase in viscosity.
- (c) The Reynolds number at which viscous effect become negligible is dependent on the Froude number; the higher the Froude number the greater is the limit of Reynolds number for freedom from viscous influences.
- (d) It was suggested that for vortex studies a geometrically similar model be constructed and operated at the same Froude number as in the

prototype. Similarity of circulation is therefore ensured by geometric similarity.

- (e) The relationship between the critical vortexing water level and the Froude number is in general as the following,

$$h/d = m (Fr)^n$$

where

m = a constant which accounts for the circulation effect.

n = a constant

Both m and n are geometric dependent.

#### 4.4.2 Test Modeling

Three criteria are used in modeling the test article:

- (a) geometric similarity
- (b) Froude number in the test model is the same as that in the plant, and,
- (c) Weber number in the test and the plant is greater than 120

Standard transparent acrylic material is used to construct the test article for visual inspection of vortex formation. A 7.0 inch inside diameter acrylic pipe is used to simulate the plant hot leg of 31 inch inside diameter, resulting a linear geometric scale of 0.226. Consequently, the test model simulate RHR pipe inside diameter is scaled to be 1.98 inches (plant RHR pipe inside diameter is 8.75 inches) and a standard acrylic pipe of 2.0 inch inside diameter is used.

The modeling criteria (a) above is satisfied by making the test model geometry the same as the plant. Particularly, the interface geometry between components is properly modeled.

The modeling criteria (b) above is automatically satisfied when the same Froude number used in the test is also used in the plant.

The relations between RHR discharge flow rate, RHR pipe inside diameter, and velocity in the plant and model situations are as follows, using a constant Froude number.

$$(Fr)_{\text{model}} = (Fr)_{\text{plant}}$$

$$(Fr) = \frac{v}{(gd)^{0.5}}$$

$$= \frac{40}{(\pi)(g^{0.5})(d^{2.5})}$$

By equating the test model Froude number to the plant Froude number, the following equations are derived.

$$Q_{\text{model}} = \left(\frac{d_{\text{model}}}{d_{\text{plant}}}\right)^{2.5} (Q_{\text{plant}})$$

and

$$\frac{d_{\text{model}}}{d_{\text{plant}}} = 0.226 \text{ ----- (a)}$$

Therefore,

$$Q_{\text{model}} = 0.024 Q_{\text{plant}} \text{ ----- (b)}$$

Similarly,

$$V_{\text{model}} = 0.475 V_{\text{plant}} \text{ ----- (c)}$$

where

$d_{\text{model}}$  = test model simulate RHR pipe inside diameter

$d_{\text{plant}}$  = plant RHR pipe inside diameter

$Q_{\text{model}}$  = test model simulate RHR pipe discharge flow rate

$Q_{\text{plant}}$  = plant RHR pipe discharge flow rate

$V_{\text{model}}$  = test model simulate RHR pipe or step nozzle flow velocity

$V_{\text{plant}}$  = plant RHR pipe or step nozzle flow velocity

For a selected Froude Number (fluid velocity), the resulting Weber number is evaluated and compared against the value given in criterion (c). The minimum flow velocity is dependent upon the test model configuration. The following summarizes the minimum flow velocity for each test model configuration. It should be pointed out that above the minimum flow velocity the flow surface tension has negligible effect on the critical vortexing water level.

For a 2.0 inch ID straight through simulated RHR pipe mounted at the bottom of the simulated hot leg the minimum flow velocity is 1.363 ft/sec. The equivalent flow rate is 13.35 gpm.

For a  $\left[ \quad \right]^{a,b}$  inch ID step nozzle mounted at the bottom of the simulated hot leg the minimum flow velocity is  $\left[ \quad \right]^{a,b}$  ft/sec. The equivalent flow rate is  $\left[ \quad \right]^{a,b}$  gpm.

For a  $\left[ \quad \right]^{a,b}$  inch ID step nozzle mounted at the bottom of the simulated hot leg the minimum flow velocity is  $\left[ \quad \right]^{a,b}$  ft/sec. The equivalent flow rate is  $\left[ \quad \right]^{a,b}$  gpm.

a, b

Figure 4.1-1 Simulated RHR Installed with Cruciform





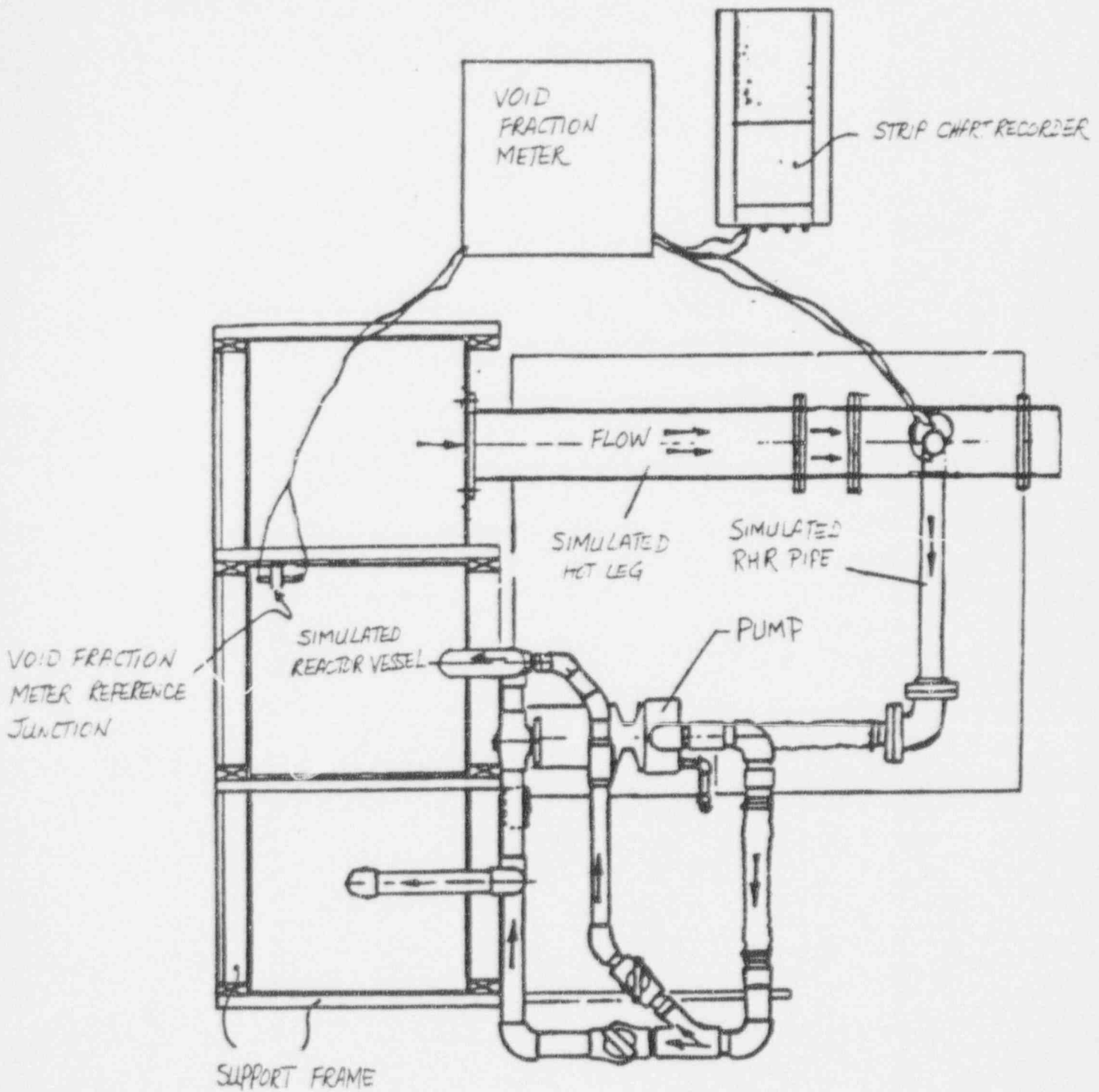


Figure 4.2-1 Test Model General Assembly - Sheet 1  
(Top View)

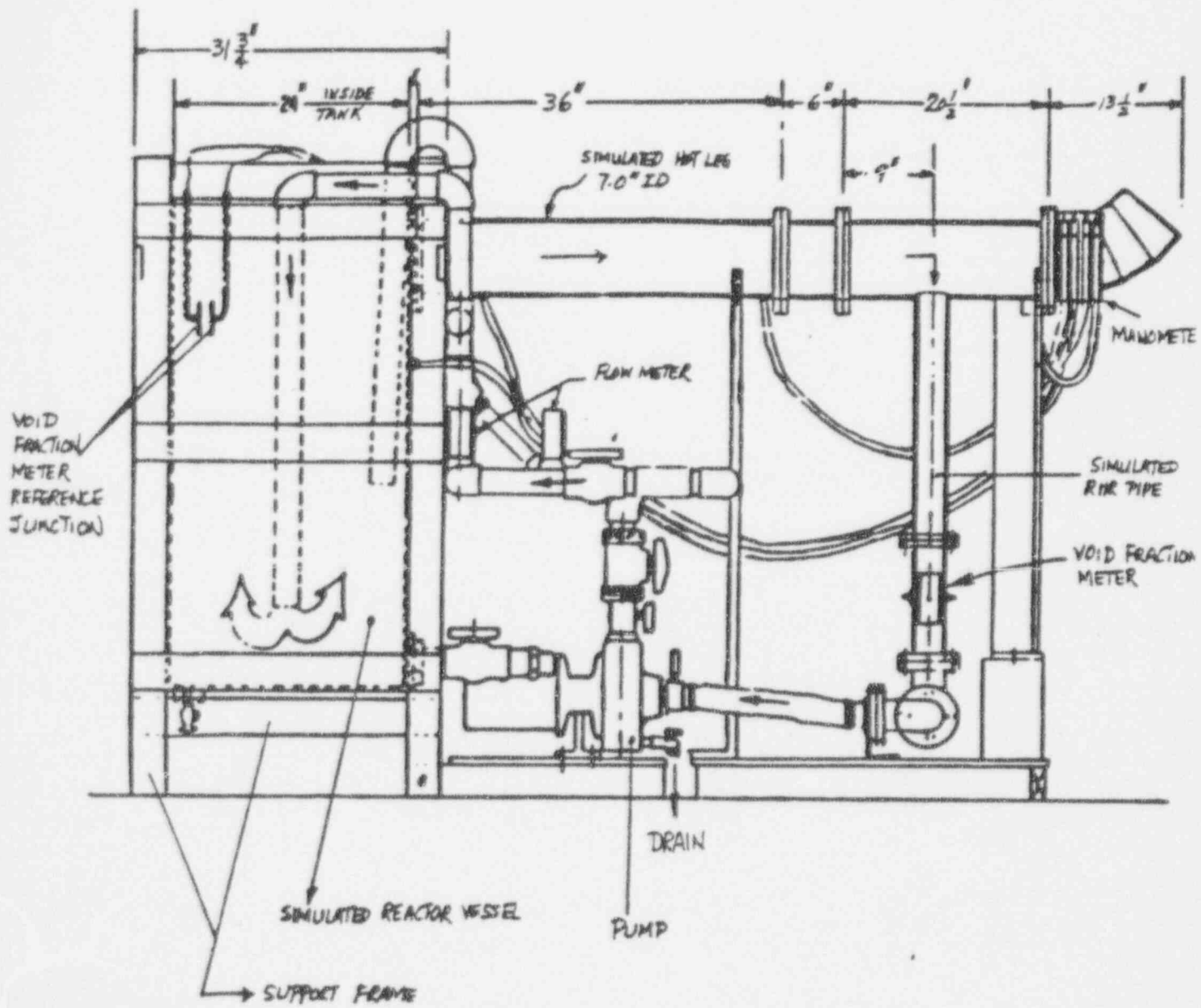
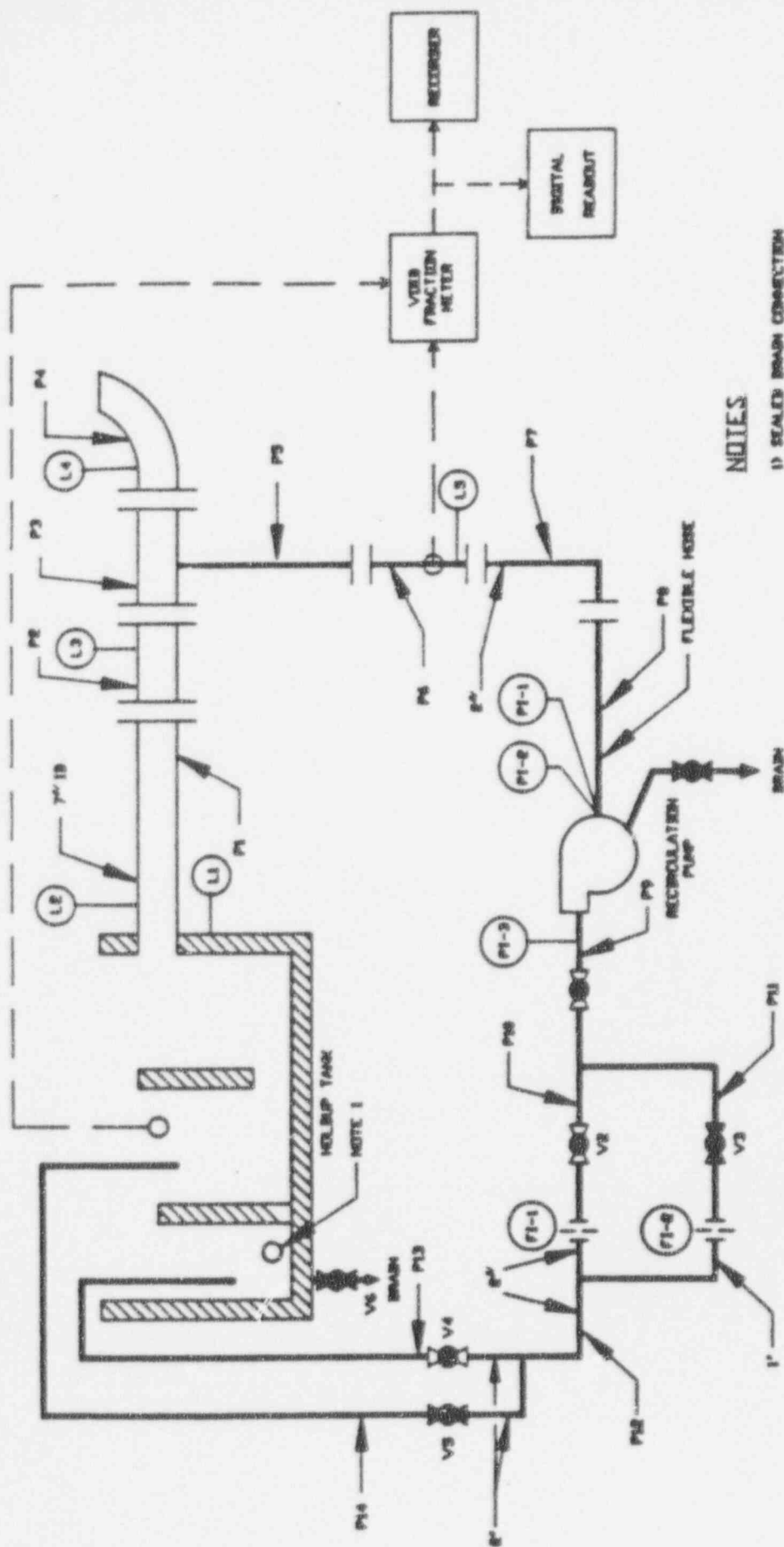


Figure 4.2-1 Test Model General Assembly - Sheet 2  
(Front View)



**NOTES**

1) SEALED BRAIN CONNECTION

**FIGURE 4.2-2**  
**TEST SYSTEM FLOW DIAGRAM**

PL RA021  
03/21/66

TABLE 4-1

EQUIPMENT PARAMETER SUMMARY

Holdup Tank

Dimensions

Height 48"  
 Width 24"  
 Length 71.5"

Material

Polypropylene

Other

Baffles divide into three sections

Main Loop Piping (Segments Pipe P2)

Dimensions

Inside Diameter 7"  
 Outside Diameter 7.5"  
 Length 76"

Spool Piece (Segment P3 and P5)

Dimensions

Main Loop Piping Section (P3)

Inside Diameter 7"  
 Outside Diameter 7.5"  
 Length 6"

RHR Suction Piping

(P5)  
 Inside Diameter 3.00"

Recirculation Pump

Type

Horizontal Centrifugal

Design Flow

103 gpm

Design Head

30 feet

Manufacturer

Grander-Teel

Model Number

1P897

Valves (V1 through V5)

Type

Ball Valves

No of Valves

5

Sizes of Valves

Four Valves

2"

One Valve

1"

## 5.0 DESCRIPTION OF TEST OPERATIONS

Descriptions of the various hot leg/RHR line interfacing geometries tested are given in Section 4.2, Test Model Description. Testing was performed over a range of simulated RHR intake flow rates to both bound possible operating conditions for the AP600 and allow for comparison of the data base developed from the current test program to other experimental data.

The general sequence of events that occurred in process of testing were:

- (1) Perform the calibration of the void meter; set outputs of electronics with meter empty (totally voided) and full of water (no voids).
- (2) Perform strip chart recorder calibration.
- (3) Fill tank and hot leg simulation to desired initial level.
- (4) Start pump; set desired flow rate through RHR line simulation.
- (5) Record the following data:
  - (a) Intake flow rate.
  - (b) Tank water level.
  - (c) Water level in hot leg simulation (three locations).
  - (d) Pump suction Pressure.
  - (e) Pump discharge pressure.
  - (f) Void fraction as measured in RHR line simulation.

The void fraction was continuously recorded for a given test run using the strip chart recorder. Duration of a test run was at least one (1) minute, up to as much as fifteen (15) minutes.

- (6) Water level in the simulated hot leg was then decreased by draining through the pump until the desired level for the next test run was achieved.
- (7) Step 5 and 6 were repeated for a given flow rate until either excessive voids were being ingested into the RHR line simulation, or the vortex at the hot leg/RHR line junction was broken.
- (8) Steps 3,4,5, and 6 were then repeated for other flow rates to be tested.

The test program was also recorded on video tapes.

## 6.0 DISCUSSION OF TEST RESULTS

The hardware configurations tested can be grouped as follows:

- (a) Simulated RHR pipe is connected directly to the bottom of the simulated hot leg.
- (b) Simulated RHR pipe is connected to the bottom of the simulated hot leg, and a cruciform is installed inside the simulated RHR pipe.
- (c) Simulated RHR pipe is connected to the bottom of an intermediate pipe, which is connected to the bottom of the simulated hot leg.

The test results obtained using these hardware configurations are discussed in this section. Table 6.1 summarizes the critical vortexing water level for all flow rates and piping arrangements.

The following sections discuss the test results in detail.

### 6.1 SIMULATED RHR PIPE CONNECTED TO BOTTOM OF SIMULATED HOT LEG

The first series of tests were run with a 2.0" ID pipe connected to the simulated hot leg of 7.0" ID. The 2.0" ID pipe corresponds to AP600 10" schedule 140 RHR pipe, and the 7.0" ID simulated hot leg corresponds to AP600 hot leg of 31" ID. The equivalent AP600 RHR flow rate of 2000 gpm is 49 gpm in the test. These test results are used as baseline information and will be used to compare with other test results.

Figure 6.1 plots these test results on a log-log scale. The Froude number, a dimensionless parameter, is defined as

$$Fr = \frac{v}{(gd)^{0.5}}$$

where Fr = Froude number

v = flow velocity at the intake pipe, ie the RHR pipe

$g$  = gravitational acceleration

$d$  = inside diameter of the intake pipe, ie the RHR pipe

Another dimensionless parameter,  $h/d$ , is plotted in Figure 6.1 as a function of  $Fr$ , where  $h$  is the water level with respect to the bottom of the inside diameter of the simulated hot leg.

Two  $h/d$  vs.  $Fr$  lines are plotted in Figure 6.1. The one on the top represents the water level, with respect to the bottom of the hot leg ID, at which a dimple begins to form at the hot leg water surface. The bottom line represents the critical vortexing water level below which air would be drawn through the simulated RHR pipe to the pump. It should be pointed out that at this critical vortexing water level, vortex has already formed at the hot leg water surface. However, its momentum is not strong enough to enable it to pass down to the simulated RHR pipe.

It was observed during testing that once the water level drops below the critical vortexing water level, the system became very unstable with erratic and high percentage of air entrainment at the pump. Figure 6.2 and Figure 6.3 are some examples of this phenomenon.

The vortex formation process was observed to be the same for all tests. A dimple formed at a certain water level. As the water level in the simulated hot leg continued to drop, at a constant flow rate at the pump, more and more dimples formed. Eventually, these dimples were replaced by a vortex. The vortex circulated counter-clockwisely and its momentum got stronger as the water level dropped lower. When the water level was dropped to below the critical level, the vortex rushed down to the pump rapidly, resulting erratic pump operation and unstable system.

The critical vortexing water level is important because it is the threshold for an unstable system. Figure 6.1 shows two straight lines for the critical vortexing water level. The knee between these two straight lines is approximately at  $Fr=1.2$ . The existence of the knee is unexpected, since all available literature predicts only one straight line. However, the



test data clearly show the existence of the knee. Furthermore, other engineers at the System Engineering Department conducted similar tests, using the same test setup and different simulated RHR pipe sizes at different orientations. Their test results show the existence of the knee also. These test results will be compared with the result of this test program in a later Section 6.4.

The data of Figure 6.1 suggests the following equations for the prediction of critical vortexing water at different flow rates for the AP600 plant.

$$\begin{array}{ll} h/d = 1.44 (Fr)^{0.28} & 1.2 \leq Fr \leq 5.0 \\ h/d = 1.33 (Fr)^{0.76} & 0.5 \leq Fr \leq 1.2 \end{array}$$

It should be pointed out that a test with a Froude number of 0.44 (10 gpm in the test or 410 gpm in the plant) was also conducted. No air entrainment at the pump was recorded even when the water level was drained to the bottom of the simulated hot leg. The corresponding Weber number is 67.2. Section 4.4.1 states that the surface tension has no influence on the critical vortexing water level when the Weber number is greater than 120. The result of this particular test supports this statement indirectly.

Presently, the RHR flow rate for AP600 is 2000 gpm for this particular configuration; and the equivalent Froude number is 2.2. The predicted critical vortexing water level, using the first equation above, is 15.89 inches. This predicted water level is only 0.39 inches higher than the mid-loop of the hot leg (15.5 inches) in the plant. Therefore, it is not acceptable to locate the RHR pipe at the bottom of the hot leg if the RHR flow rate is 2000 gpm or higher for mid-loop operation.

## 6.2 SIMULATED RHR PIPE CONNECTED TO BOTTOM OF HOT LEG WITH CRUCIFORM INSTALLED INSIDE SIMULATED RHR PIPE

Prior to the design of this test program, a study was conducted to investigate the parameters that would affect the vortexing phenomenon. (Reference 4) Two

parameters were found to be very important, namely, the circulation effect and the water level of the inventory. (ie, the RCS hot leg water level in the plant)

The circulation effect can be reduced or minimized by locating the RHR pipe at an angle of 45 degrees above the bottom of the hot leg. There have been tests conducted addressing this 45 degree RHR pipe configuration before. The test results will be compared later in Section 6.4.

The second series of this test program used a cruciform installed inside the simulated RHR pipe which was located at the bottom of the simulated hot leg. The cruciform was thought to be an effective vortex breaker by minimizing or breaking up the circulation effect.

The results of this test series are compared with those of the first series of tests. Figures 6.4 and 6.5 compare the test results. It should be pointed out that 49 gpm in the test is equivalent to 2000 gpm in the plant. Figure 6.4 shows that at 49 gpm the percentage of air entrainment in the pump is worse with the cruciform than without the cruciform at the same water level. Also the cruciform configuration is more unstable with more frequent high percentage of air entrainment. Figure 6.5 shows similar results at a higher flow rate.

These test results were unexpected as it was presumed that the cruciform would breakup the vortex. However, it was observed during testing that the cruciform did not breakup the vortex; instead, it channeled the vortex. Moreover, the cruciform decreased the flow area in the RHR nozzle simulation resulting a higher flow velocity in that region and a more rapid vortexing rate.

The corresponding Froude number at the cruciformed area is actually higher than that without the cruciform. Section 6.1 points out that the critical vortexing water level is directly proportional to the Froude number raised to a power of  $[ ]^{a+b}$ . Therefore, the critical vortexing water level for the cruciformed configuration is actually higher than that without the cruciform. The data given in the following table supports this conclusion.

Test Flow Rate (GPM)	Measured Critical Vortexing Water Level	
	With Cruciform	Without Cruciform
107	[ ] <sup>a,b</sup> inches	[ ] <sup>a,b</sup> inches
49	[ ] inches	[ ] inches

Since the cruciform does not breakup the circulation and, for a given RHR line size, it raises the critical vortexing water level, it is not a viable design.

### 6.3 AN INTERMEDIATE PIPE AT BOTTOM OF HOT LEG AND RHR PIPE AT ITS BOTTOM

The third series of the test program used an intermediate size pipe (a step nozzle) connected to the bottom of the hot leg. Figure 4.1-2 shows the physical arrangements. The size of each arrangement is listed below.

Intermediate Pipe Inside Diameter		Intermediate Pipe Length	
Test Model	AP600 Plant	Test Model	AP600 Plant
[ ] <sup>a,b</sup>			

The simulated RHR pipe of 2.0 inches in inside diameter was connected to the bottom end of each of these intermediate size pipe.(step nozzle)

The reasons for this arrangement are two folds:

- (a) The intermediate pipe (step nozzle) becomes an integral part of the hot leg, ie, it increases the water inventory to some degree. Consequently, the available water level is effectively increased. This parameter has major influence on the formation of vortex at a given flow rate.

(b) Contrary to the cruciform arrangement, the use of the intermediate size pipe increases the flow area resulting with a smaller intake velocity. Consequently, the corresponding Froude number is smaller - another parameter that has major influence on the formation of vortex at a given flow rate.

This step nozzle concept was first proposed in Reference 4 and it is further suggested by the test results of the first test series.

The following sections discuss the test results in details.

Arrangement 1  $\left[ \begin{array}{c} a, b \\ \text{---} \\ \text{---} \\ \text{---} \end{array} \right]$  Inch Step Nozzle By 12 Inch Length

Figure 6.6 compares the test results of the  $\left[ \begin{array}{c} a, b \\ \text{---} \\ \text{---} \\ \text{---} \end{array} \right]$  inch ID intermediate pipe with that of the 2.0 inch ID straight through simulated RHR pipe. It is clear from comparison the figure that the h/d ratio for the  $\left[ \begin{array}{c} a, b \\ \text{---} \\ \text{---} \\ \text{---} \end{array} \right]$  inch intermediate pipe arrangement is smaller than that of the 2.0 inch ID simulated RHR pipe.

The predicted critical vortexing water levels for these two configurations in the plant are compared as follows:

AP600 Plant With Straight Through RHR Pipe At The Bottom  
Of The Hot Leg. Its Critical Vortexing Water Level -----  $\left[ \begin{array}{c} a, b \\ \text{---} \\ \text{---} \\ \text{---} \end{array} \right]$  inches

AP600 Plant With  $\left[ \begin{array}{c} a, b \\ \text{---} \\ \text{---} \\ \text{---} \end{array} \right]$  Inch ID Intermediate Pipe And 53.1  
Inches In Length. Its Critical Vortexing Water Level -----  $\left[ \begin{array}{c} a, b \\ \text{---} \\ \text{---} \\ \text{---} \end{array} \right]$  inches

This arrangement, with the critical vortexing water level being lower than the mid-loop water level of 15.5 inches in the plant, is desirable for the mid-loop operation with very low margin.

Figure 6.7 shows the percentage of air entrainment at the suction of the simulated RHR pump as a function of the water level in the simulated hot leg. The test flow rate is 49 gpm (2000 gpm in the plant). It shows that when the water level is high enough there is no air drawn through the simulated RHR

pipe. As the water level drops to a certain level, a dimple forms. More and more dimples form until they combine together as a vortex circulating counter-clockwisely. When the water level drops below the critical vortexing water level, the vortex gains enough momentum to pass through the simulated RHR pipe and cavitates the pump. This vortexing process is very much the same as that of the straight through simulated RHR pipe case. The differences between them are:

- a) The intermediate pipe lowers the critical vortexing water level
- b) The intermediate pipe arrangement is a much more stable and predictable system from the vortexing point of view. Comparison of Figure 6.3 and Figure 6.7 shows that when the water level drops below the critical vortexing water level, the air fraction by volume entrained in the pump for the intermediate pipe arrangement is far less than that of the straight through simulated RHR pipe arrangement.
- c) An interesting phenomenon occurred when the water level dropped below the critical vortexing water level. Figure 6.7 shows that the vortexing operation changed into pure spill and fill mode of operation once the water levels dropped to approximately 2.23 inches in the test (or 9.87 inches in the plant). The air entrainment at the pump is significantly reduced and the system becomes much more stable. This change did not occurred in the first two series of tests.

Although the [ ]<sup>a, b</sup> inch intermediate pipe arrangement is acceptable for the mid-loop operation, there are two drawbacks that make this design undesirable. The first drawback is that the margin for the mid-loop operation is approximately [ ]<sup>a, b</sup>. It is desirable to have a larger safety margin - as large as practicably achievable. The second drawback is that the intermediate pipe is relatively too long in the plant (53.1 inches). It is desirable to use as short an intermediate pipe as possible. Consequently, intermediate pipe of larger size and different lengths were studied.

Arrangement 2 - [ ]<sup>a,b</sup> Inch Intermediate Pipe And 12 Inches In Length

The results of the first series of tests (2.0 inch straight through simulated RHR pipe) suggested a low Froude number, and the [ ]<sup>a,b</sup> inch ID step nozzle test result hinted a larger step nozzle. The optimal step nozzle size was then estimated using test results of the straight through nozzle tests.

From the first series of tests, it was determined that when the Froude number drops to approximately 0.44, the Weber number is less than 120 and the surface tension becomes an important factor. The optimal step nozzle was sized by selecting the step nozzle inside diameter to get a Froude number of [ ]<sup>a,b</sup> at 49 gpm (or 2000 gpm in the plant), and it was calculated to be [ ]<sup>a,b</sup> inches in inside diameter. Consequently, a standard plastic pipe of [ ]<sup>a,b</sup> inch ID was used for the test.

Figure 6.8 plots the h/d ratio as a function of the Froude number. It should be pointed out that the reference zero for the water level h is at the bottom of the hot leg ID, and d is the inside diameter of the intermediate pipe [3.86]<sup>a,b</sup> inches test model or [ ]<sup>a,b</sup> inches plant). Figure 6.8 shows that all the data points are very linear on the log-log scale. The water level at which the dimple begins to form is governed by the following equation:

$$h/d = [ ]^{a,b}$$

The critical vortexing water level is governed by the following equation:

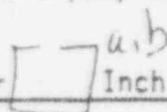
$$h/d = [ ]^{a,b}$$

This equation is used to predict the critical vortexing water level in the plant with similar geometry. The plant RHR flow rate is currently set at 2000 gpm (Froude number = 0.42) and the corresponding critical vortexing water level is [ ]<sup>a,b</sup> inches above the bottom of the hot leg inside diameter. When compared to the mid-loop operation water level of 15.5 inches, this arrangement represents an improvement of [ ]<sup>a,b</sup>

Figure 6.9 provides the percentage of air entrainment in the simulated RHR flow as the water level drops and the pump runs at 49 gpm (2000 gpm in the plant). The vortex formation process was observed in the test to be similar to the first two test series, but at a lower water level. Figure 6.9 shows a major benefit of this particular arrangement. The system is extremely stable and predictable even when the water level drops below the critical vortexing water level; and the vortexing phenomenon is replaced by pure spill and fill type of operation. The corresponding air entrainment at the pump was measured to be 1 to 2 percents, and the average value being 1.5 % air by volume.

In summary, this geometrical arrangement is desirable for the following reasons:

- (a) It has a low critical vortexing water level, much lower than the mid-loop level.
- (b) Even when the water level drops below the critical vortexing water level, the system is still very stable and predictable, with negligible pump cavitation.

Arrangement 3 -  Inch Step Nozzle By 5.56 Inch Length

Arrangement 2 was shown to be a desirable configuration. However, it is more desirable to shorten the step nozzle without sacrificing the benefits. This arrangement cuts the step nozzle length almost in halves.

Figure 6.10 plots the h/d ratio as a function of the Froude number. The water level at which the dimple begins to form is governed by the following equation:

$$h/d = \left[ \quad \quad \quad \right]^{a, b}$$

The critical vortexing water level is governed by the following equation:

$$h/d = \left[ \quad \quad \quad \right]^{a, b}$$

These two equations are basically the same as those of the 12 inch long step nozzle.

This arrangement predicts the critical vortexing water level in the plant to be [ ]<sup>a,b</sup> inches from the bottom of the hot leg. It is [ ]<sup>a,b</sup> inches below the mid-loop level in the plant, and it represents an improvement of [ ]<sup>a,b</sup> from the mid-loop level.

Figure 6.11 studies the percentage of air entrainment in the pump as the water level drops and the pump runs at 49 gpm (2000 gpm in the plant). Similar to arrangement 2, the system response for this arrangement is extremely stable and predictable even when the water level drops below the critical vortexing water level. The step nozzle prevents the vortex from being drawn down to the pump successfully. When the water level drops below the already low critical vortexing water level, the vortex is changed into pure spill and fill type operation - the water simply spills over from the simulated hot leg into and fills the step nozzle. The step nozzle acts as a holdup tank. As the water spills over into this holdup tank, it brings with it some air. The average percentage of this air that is drawn through the simulated RHR pipe, as shown in Figure 6.11, was measured to be approximately 5%.

In summary, this arrangement with a step nozzle of [ ]<sup>a,b</sup> inch ID by 5.56 inch length seems to be an optimal and acceptable design.

#### Arrangement 4 - 3.86 Inch Step Nozzle By 4.3 Inch Length

This arrangement used a shorter step nozzle than that of the previous arrangement. The goal was to find out the shortest step nozzle without changing the critical vortexing water level.

Figure 6.12 plots the h/d ratio as a function of the Froude number. It shows that all the data points are very linear on the log-log scale. The critical vortexing water level is governed by the following equation:

$$h/d = [ ]^{a,b}$$



This equation is clearly different from that of the two longer step nozzles. It predicts a critical vortexing water level of  $\left[ \quad \right]^{a,b}$  inches in the plant at 2000 gpm RHR flow rate. It is about  $\left[ \quad \right]^{a,b}$  inches below the mid-loop level of the hot leg, or an improvement of  $\left[ \quad \right]^{a,b}$  from the mid-loop level. This improvement is even less than that of arrangement 1.

Figure 6.13 studies the percentage of air entrainment in the simulated RHR flow as the water level drops and the pump runs at 49 gpm (2000 gpm in the plant). Once the water level drops below the critical vortexing water level, the vortex gains enough momentum and passes down to the pump rapidly with relatively large amount of air. The pump becomes cavitated and the flow rate becomes unstable. However, the degree of pump cavitation is still far less severe than the 2 inch straight through simulated RHR pipe case.

Although this design is acceptable for mid-loop operation, it is not the most desirable design.

Arrangement 5 -  Inch Step Nozzle By 2.876 Inch Length

A few tests were run with this arrangement to further verify that the optimal step nozzle length is approximately 5.56 inches, ie., arrangement 3.

The critical vortexing water level at 49 gpm (2000 gpm in the plant) was measured to be approximately  $\left[ \quad \right]^{a,b}$  inches  $\left[ \quad \right]^{a,b}$  inches in the plant). This critical level is practically the same as that of arrangement 4.

Figure 6.14 studies the percentage of air entrainment in the pump as the water level drops and the pump runs at 49 gpm (2000 gpm in the plant). It can be seen from the data that the pump is highly cavitated and the system becomes very unstable, once the water level in the simulated hot leg drops below the critical vortexing water level of  $\left[ \quad \right]^{a,b}$  inches. In fact, when the water level was dropped to  $\left[ \quad \right]^{a,b}$  inches in the test  $\left[ \quad \right]^{a,b}$  inches in the plant) the flow was observed to be highly unstable. The pump was stopped to prevent any damage due to erratic operations.

In summary, the third series of the test program studied parametrically the behavior of the vortex and the system performance at various water levels and flow rates with different geometrical arrangements. Based on the preceding test data, it is concluded that the optimal arrangement is the arrangement 3 - a step nozzle of  $\left[ \begin{array}{c} \text{---} \\ \text{---} \end{array} \right]_{\text{inch}}^{\text{a,b}}$  ID by 5.56 inch length, equivalent to a plant dimension of  $\left[ \begin{array}{c} \text{---} \\ \text{---} \end{array} \right]_{\text{inch}}^{\text{a,b}}$  ID by 24.6 inch length.

#### 6.4 COMPARISON WITH OTHER TESTS

This section compares the test results with similar tests performed by others in the industry or within Westinghouse.

##### 6.4.1 Comparison With Mitsubishi Heavy Industries Test

Takasage Research Laboratory of Mitsubishi Heavy Industries has performed tests to model RHR partial-loop operations. The MHI test model was developed using the first two criteria of this test program, i.e., the geometric similarity was preserved and the Froude number was modeled. Tests were performed with (1) the RHR nozzle connected to the bottom of the hot leg, and (2) the RHR nozzle connected to the hot leg at 45 degrees from the bottom of the hot leg. The following general conclusions were made:

- (a) Virtually all air contained in the vortex would flow along with water rapidly when the Froude number is greater than 1.0.
- (b) Only a small portion of the air in the vortex would flow along with water when the Froude number is less than 1.0
- (c) In the case where the RHR nozzle is connected to the hot leg at a 45 degree angle from the bottom of the hot leg, the critical vortexing water level can be predicted by

$$h/d = 1.55 (Fr)^{0.59}$$

(d) When the RHR nozzle is connected to the bottom of the hot leg, the critical vortexing water level can be predicted by

$$h/d = 2.5 (Fr)^{0.636}$$

The MHI's conclusions (a) and (b) are supported by this test program. However, This test program further indicates that no air would travel with the water when the Froude number is much less than 1.0. ie, when the Weber is less than 120.

No comparison can be made between this test program and conclusion (c) above due to differences in test model geometry.

The data of the current test program does not support MHI's conclusion (d) above. It seems that MHI has missed the knee point that separates the equation into two straight lines of different slopes. Figure 6.15 compares the test results. All data points for MHI tests are read directly from the MHI's test report; and they are actual test data points. W's interpretation of the data are plotted as two solid lines; and the MHI's is the broken line. Perhaps the main reason for this difference in data interpretation is the data point where Fr is 0.41 and h/d is 1.41. If this data point is disregarded, the existence of the knee point becomes clear.

Figure 6.15 also shows that MHI predicts a higher\* critical vortexing water level at a given flow rate than the W's prediction. Two major factors contribute to this difference:

- (a) For air volume measurement MHI used a hot wire anemometer, whereas W used an air fraction void meter. Hot wire anemometer measures air velocity directly, which then must then be used to calculate the corresponding air volume. The air fraction void meter used by W measures directly the air volume and it can be calibrated in place. Consequently the measurement using the void meter is more accurate.

(b) There is a slight difference in the definition of critical vortexing water level used by MHI and W. MHI defines the critical vortexing water level as the hot leg water level at which the vortex begins to pass down to the RHR nozzle. W defines the critical vortexing water level as the hot leg water level at which the air fraction void meter actually records 0 to 0.5 percent of air by volume passing down to the pump. The air fraction void meter was located just upstream of the pump.

#### 6.4.2 Comparison With Other Westinghouse Test

Westinghouse Owners Group (WOG) sponsored a test program using the same test facility with different hot leg and RHR nozzle combinations. RHR nozzles of different sizes and orientations were tested. WOG's test used the same air fraction void meter at the same elevation as that of this test program. Some of the tests used (1) RHR nozzles of different sizes each located at the bottom of the hot leg, and, (2) RHR nozzles of different sizes each located at 45 degrees above the bottom of the hot leg. The results are summarized as follows:

- (a) Air contained in the vortex flows along with water rapidly when the Froude number is greater than 1.0
- (b) Only a small portion of the air in the vortex flows along with water when the Froude number is less than 1.0
- (c) In the case where the RHR nozzle is connected to the hot leg at a 45 degree angle, the critical vortexing water level can be predicted by

$$\begin{array}{l}
 h/d = [ \\
 h/d = [ \quad \quad \quad ]^{a,b}
 \end{array}$$

- (d) When the RHR nozzle is connected to the bottom of the hot leg, the critical vortexing water level can be predicted by using the same equation from this test program.

Figure 6.16 show the WOG's test results with 45 degree RHR nozzle configuration. It should be noted that the reference zero water level is at the bottom of the hot leg inside diameter. It clearly shows the knee point at the proximity of a Froude number of 1.0. The exact location of the knee point is not known.

Figure 6.17 compares the data obtained from the WOG's test with this test program. The broken straight line is the line obtained from this test program (see section 6.1). The figure clearly indicates the existence of the knee point at approximately  $Fr = 1.2$ . The test results of this test program and that of the WOG's program agree very well.

#### 6.4.3 Comparison of Results With RHR Nozzle of Different Configuration

The test results of this test program and that of the WOG's program provide enough information to select the most desirable design.

For 45 degree RHR nozzle configuration, the critical vortexing water level can be predicted by

$$h/d = \left[ \quad \right]^{a,b}$$

If the RHR nozzle in AP600 is located at 45 degrees above the hot leg, the corresponding critical vortexing water level is (Froude number is 2.2 and the RHR nozzle ID is 8.85 inches) 13.78 inches above the bottom of the inside diameter of the hot leg.

For the bottom mounted RHR nozzle configuration, the critical vortexing water level is predicted by

$$h/d = \left[ \quad \right]^{a,b}$$

The corresponding AP600 critical vortexing water level is (Froude number is 2.2 and the RHR nozzle ID is 8.85 inches) 15.89 inches above the bottom of the ID of the hot leg.

For the bottom mounted RHR nozzle of 8.85 inches in inside diameter with a step nozzle of [ ]<sup>a,b</sup> inches inside diameter by 24.6 inches long, the critical vortexing water level can be predicted by

$$h/d = [ ]^{a,b}$$

The corresponding AP600 critical vortexing water level is (Froude number is 0.44 in this case) [ ]<sup>a,b</sup> inches above the bottom of the hot leg.

Based on this comparison of data from the current test program and that collected from the WOG-sponsored test, it is concluded that the step nozzle configuration is the optimal design for mitigating vortices during mid-loop operation.

## 6.5 SUMMARY

The test results are summarized as follows:

- (a) In the AP600 plant design, the bottom mounted RHR configuration is viable but undesirable due to extremely low margin, from the mid-loop operation point of view.
- (b) Installation of a cruciform inside the RHR pipe is unacceptable.
- (c) Installation of a step nozzle of larger size than the RHR pipe is highly desirable since it results with the lowest critical vortexing water level and a much more stable system.
- (d) The most optimal step nozzle configuration for the AP600 design is found to be a step nozzle of approximately [ ]<sup>a,b</sup> inches inside diameter and a length of approximately 24.6 inches. This step nozzle is mounted at the bottom of the hot leg with the RHR pipe mounted to its bottom.

TABLE 6.1

SUMMARY OF TEST AND PREDICTED PLANT RESULTS (SHEET 1)

NOTES: (1) CRITICAL VARIATIONS WATER LEVEL IS THE WATER LEVEL AT HOT LEG (WITH RESPECT TO BOTTOM OF HOT LEG ID) BELOW WHICH AIR FLOWS WITH THE FLOW TO THE PUMP & CAVITATES THE PUMP

(2) DIMPLE FORMATION WATER LEVEL IS THE WATER LEVEL AT HOT LEG AT WHICH DIMPLE BEGINS TO FORM.

(3) INTRINSIC PIPE REFERS TO EITHER THE AIR PIPE OR THE STEP NOZZLE

R. b

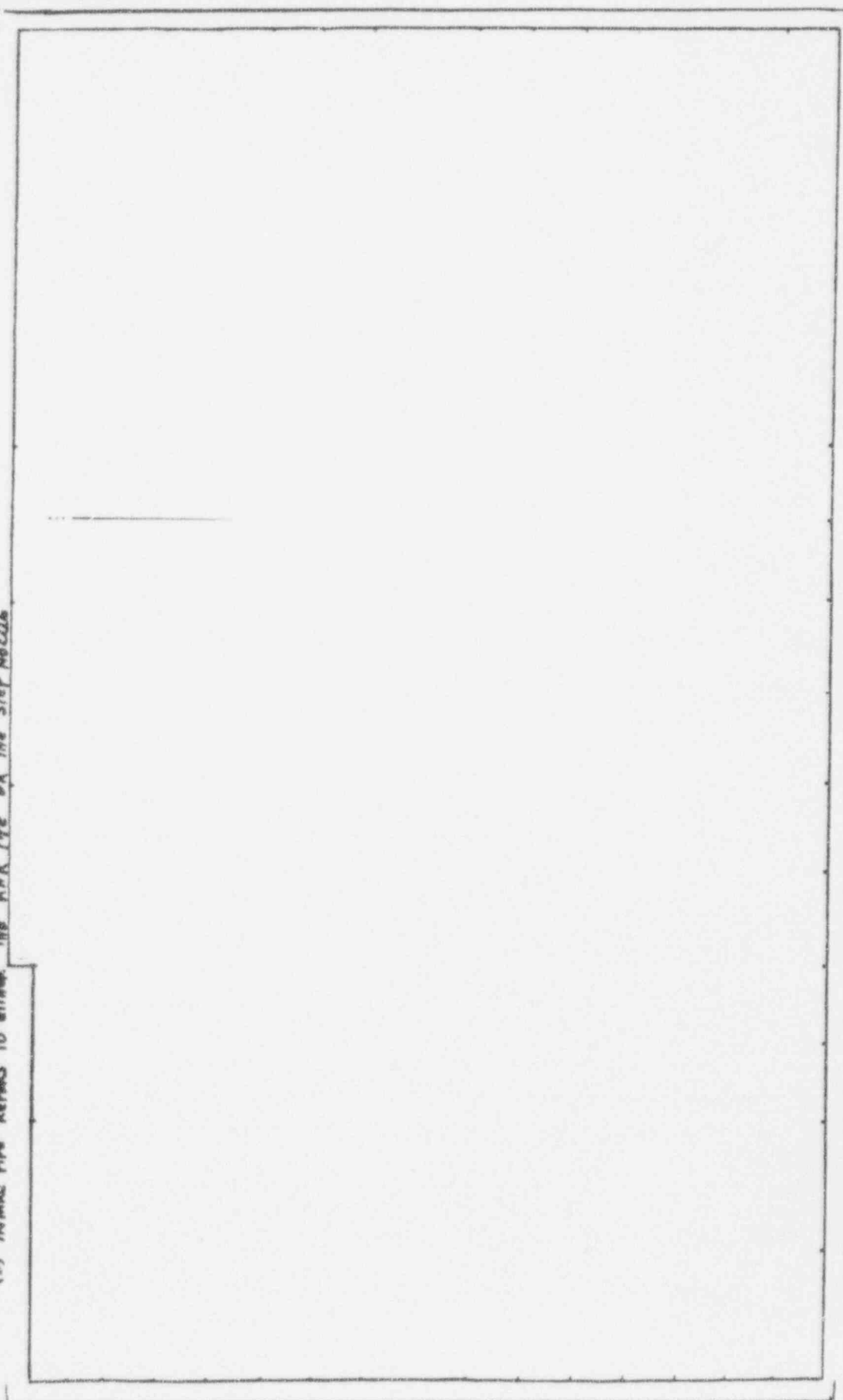


TABLE 6.1

SUMMARY OF TEST AND PREDICTED PLANT RESULTS (SHEET 2)

- NOTES: (1) CRITICAL VAPORING WATER LEVEL IS THE WATER LEVEL AT HOT LEG (WITH RESPECT TO BOTTOM OF HOT LEG ID) BELOW WHICH AIR FLOWS WITH THE FLOW TO THE PUMP & CAVITATES THE PUMP. a, b
- (2) DIMPLE FORMATION WATER LEVEL IS THE WATER LEVEL AT HOT LEG AT WHICH DIMPLE BEGINS TO FORM.
- (3) INTAKE PUMP BEGINS TO EITHER THE AIR PIPE OR THE STEP NOZZLE.

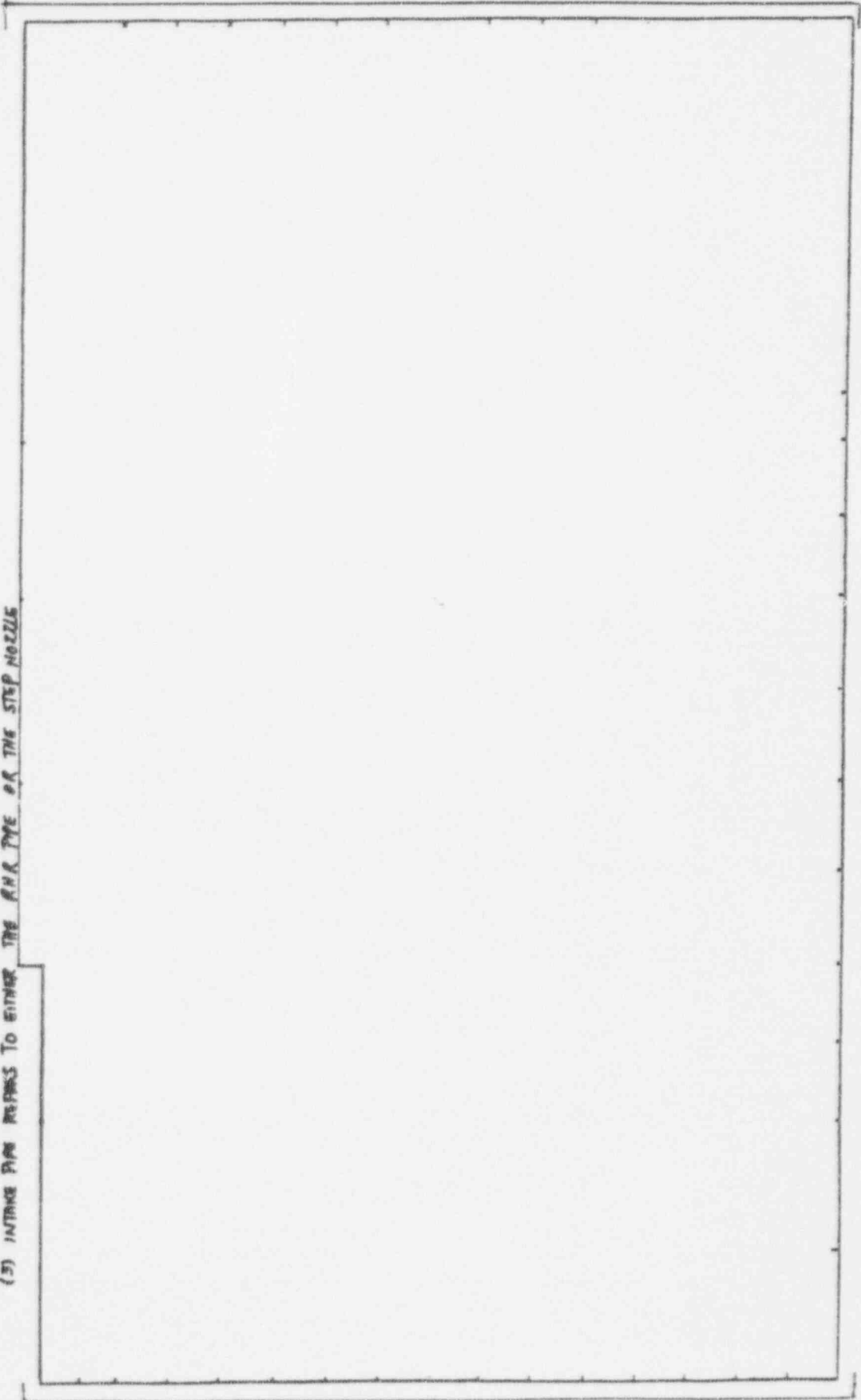




TABLE 6.1

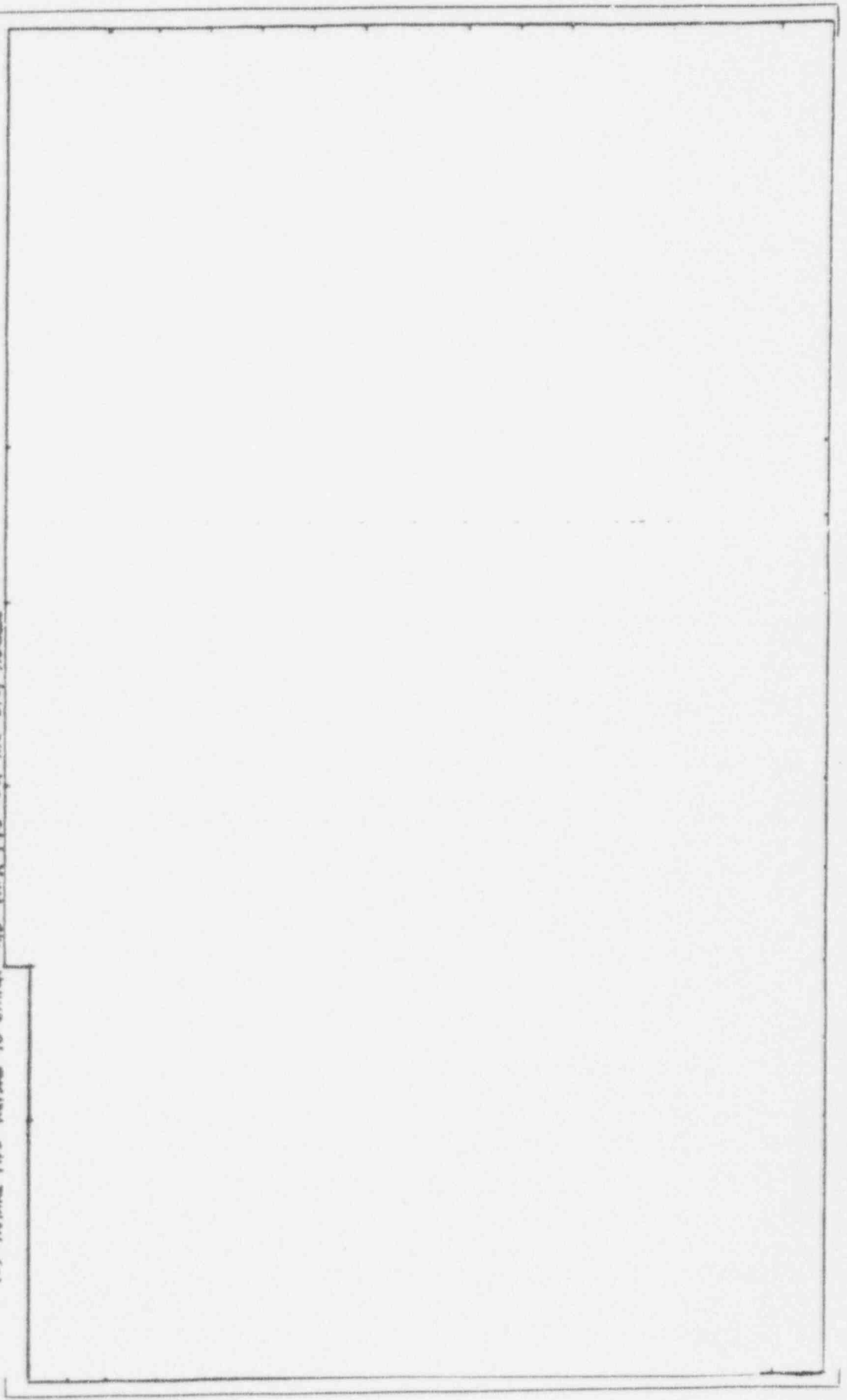
SUMMARY OF TEST AND PREDICTED PLANT RESULTS (SHEET 3)

NOTES: (1) CRITICAL VARIATIONS WATER LEVEL IS THE WATER LEVEL AT HOT LEG (WITH RESPECT TO BOTTOM OF HOT LEG ID) BELOW WHICH AIR FLOWS WITH THE FLOW TO THE PUMP & CAVITATES THE PUMP

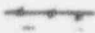

(2) DIMPLE FORMATION WATER LEVEL IS THE WATER LEVEL AT HOT LEG AT WHICH DIMPLE BEGINS TO FORM.

(3) INSTANT PIPE BEGINS TO EITHER THE AIR FLOW OR THE STEP NOZZLE

R, b



a, b

 WATER LEVEL AT WHICH DUMPLE BEGINS TO FORM AT N.L. SURFACE  
 CRITICAL LEVEL BELOW WHICH VORTEX WILL SUCK THROUGH THE PIPE TO THE PUMP

Froude Number,  $Fr = \frac{V}{\sqrt{gD}}$

NOTE: REFERENCE ZERO FOR  $h$  IS AT BOTTOM  
 @: NOT LEG ID.

Figure 6.1 Vortexing Water Level vs. Froude No.

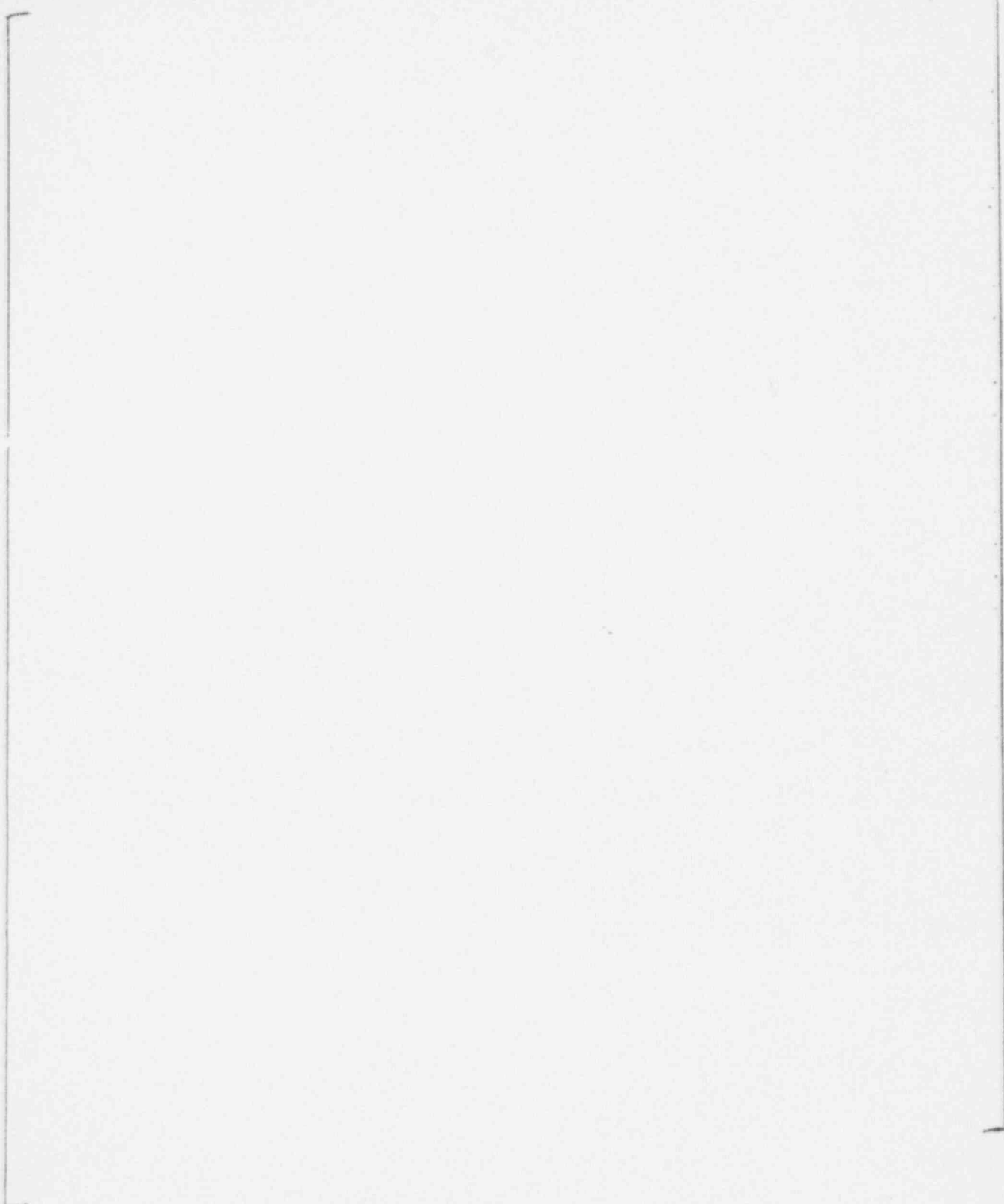


Figure 6.2 Comparison of Test Results  
(e 2.00" Simulated RHR Pipe at Bottom of Hot Leg)

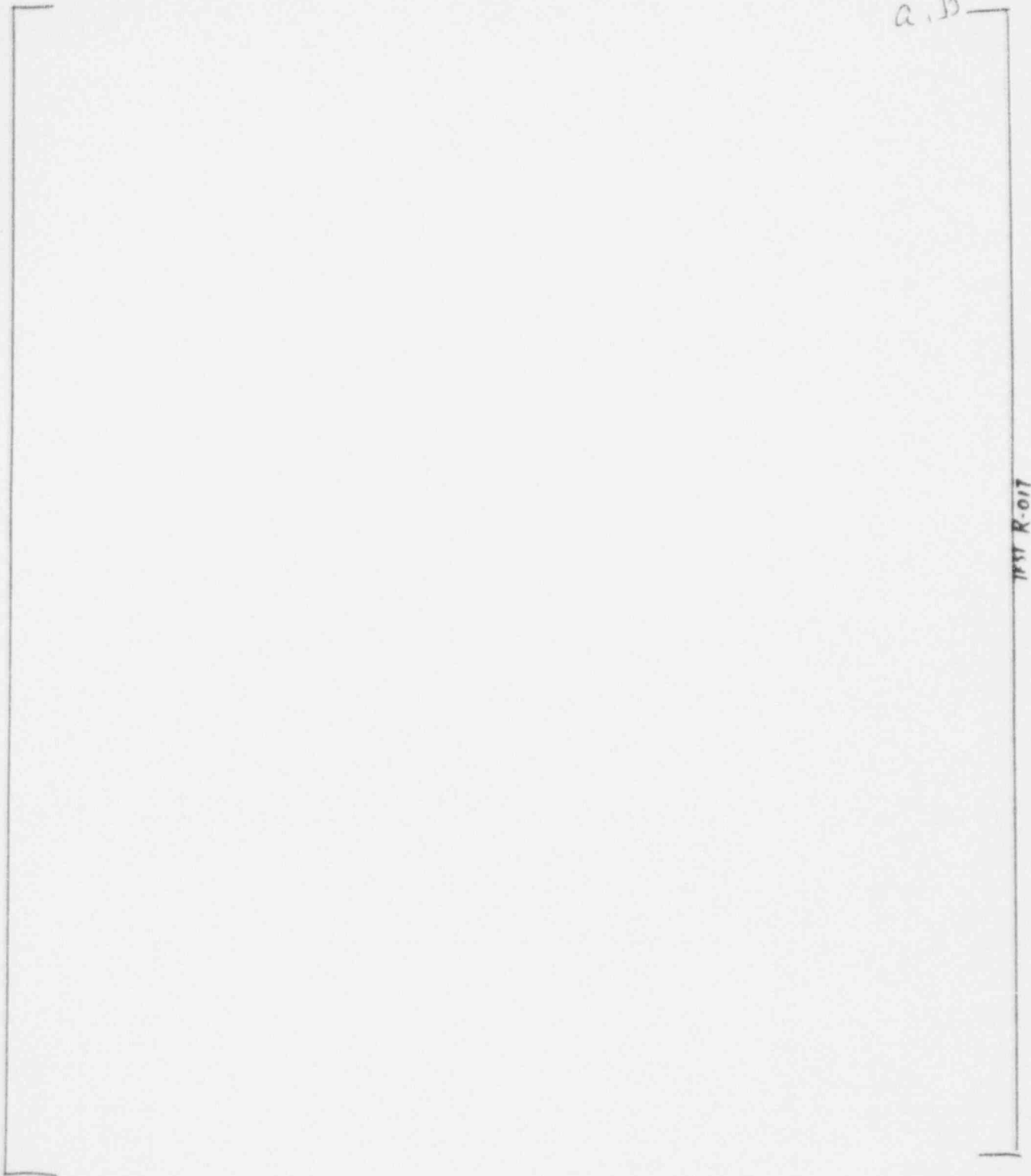
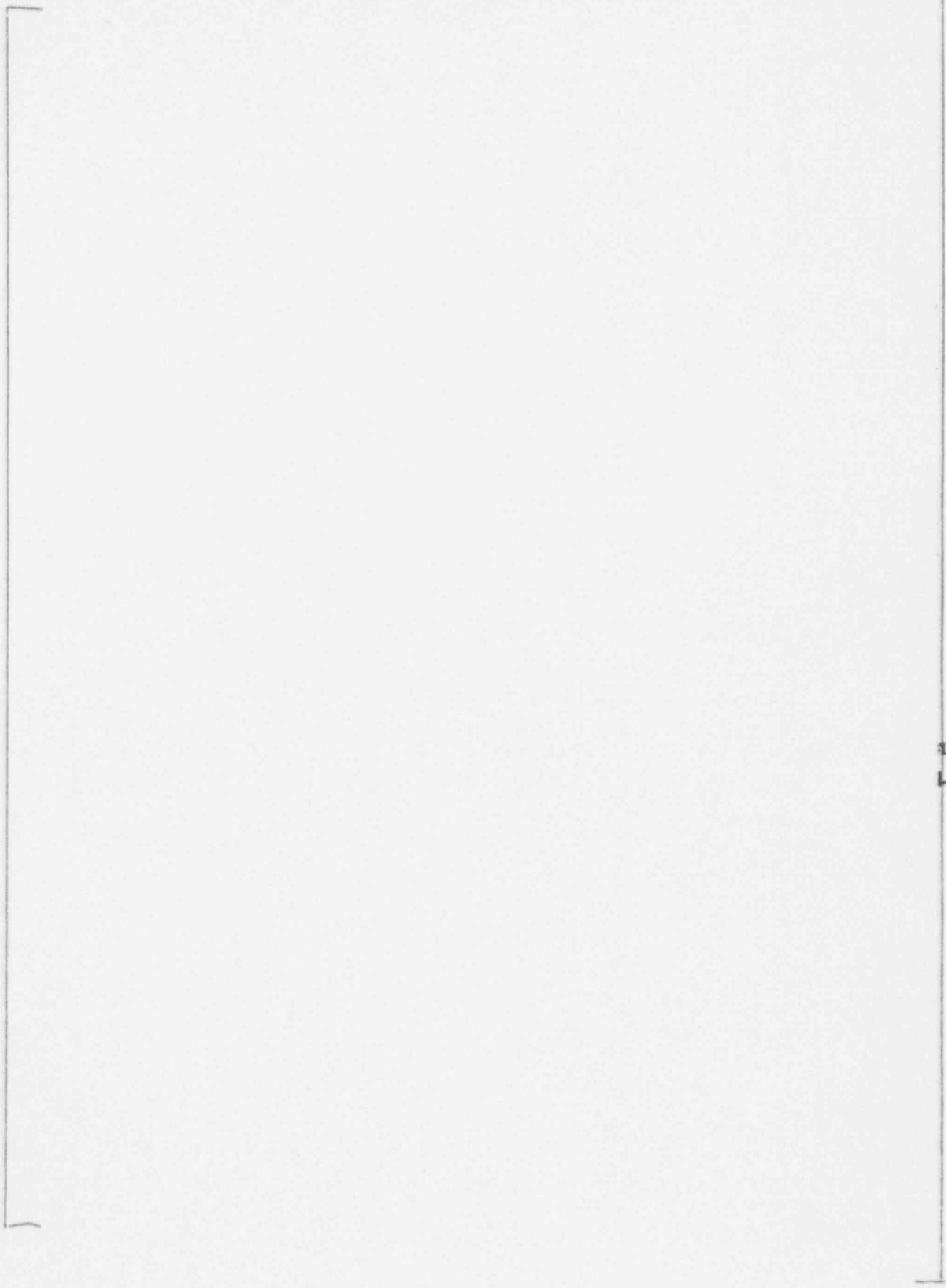


Figure 6.3 Comparison of Test Results  
( $\phi$  2.00" Simulated RHR Pipe at Bottom of Hot Leg)

Figure 6.4 Comparison of Test Results

a.b



ayb

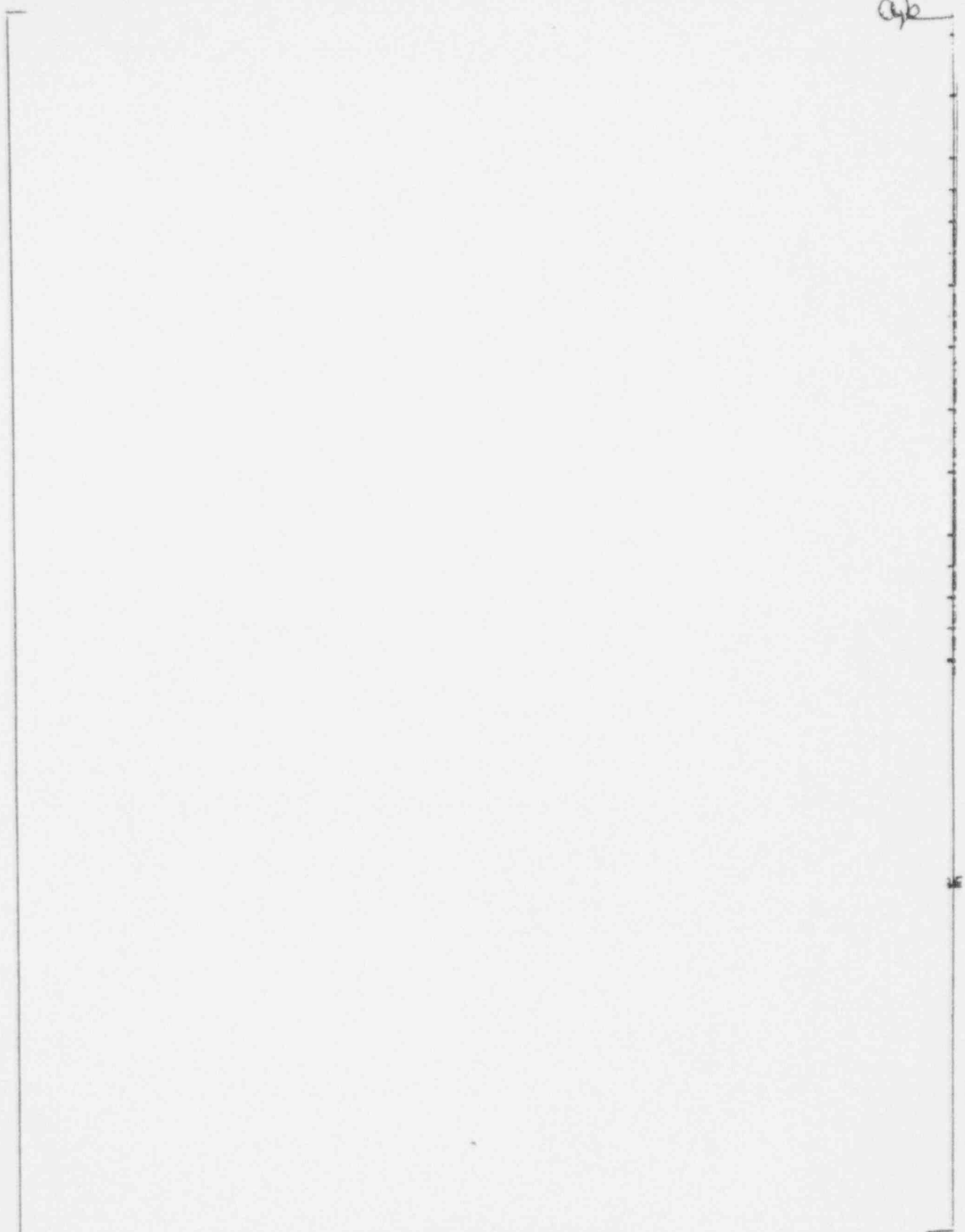


Figure 6.5 Comparison of Test Results

2, b

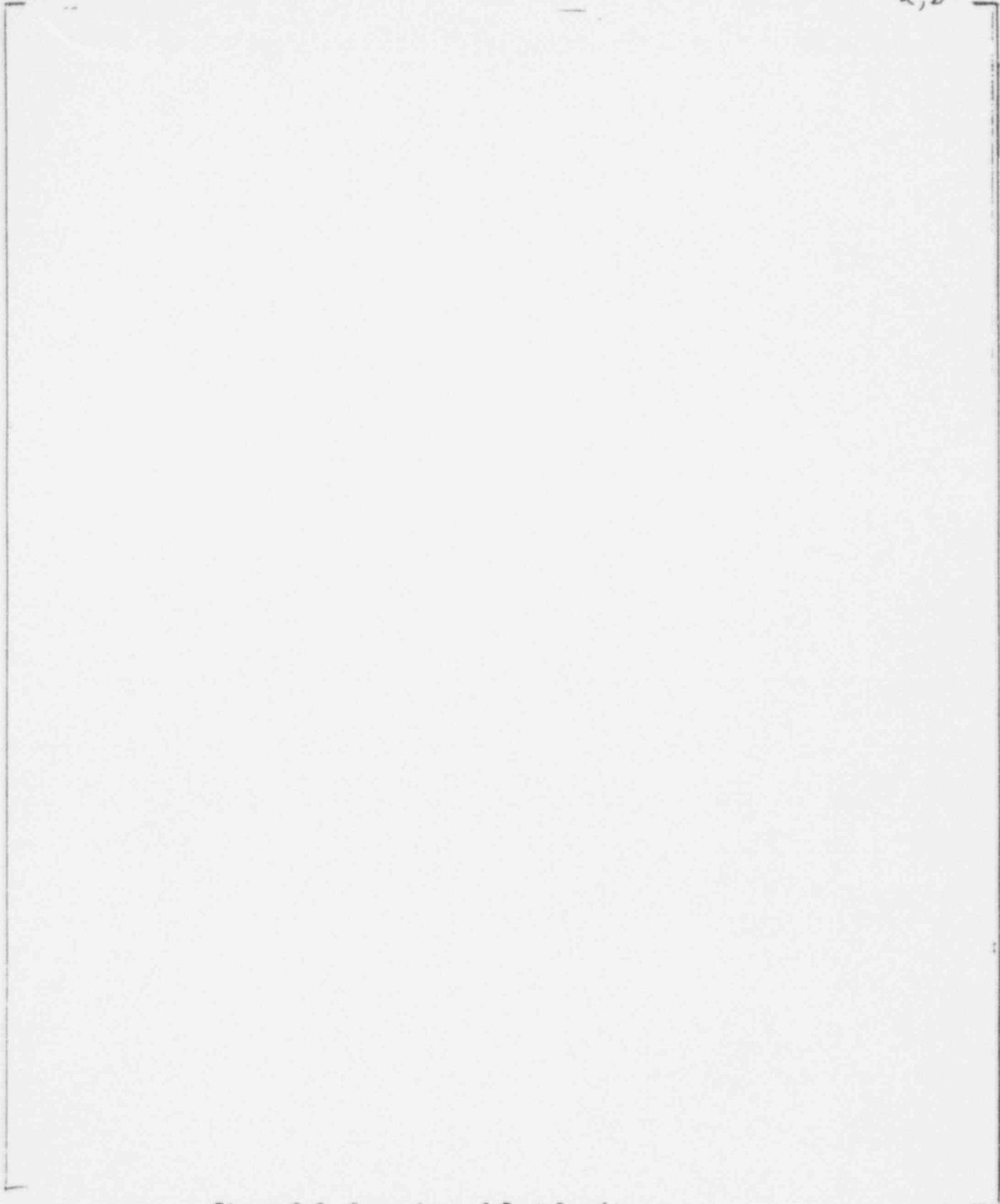


Figure 6.6 Comparison of Test Results -  
3" Intermediate Pipe vs Simulated RHR Pipe

a. b

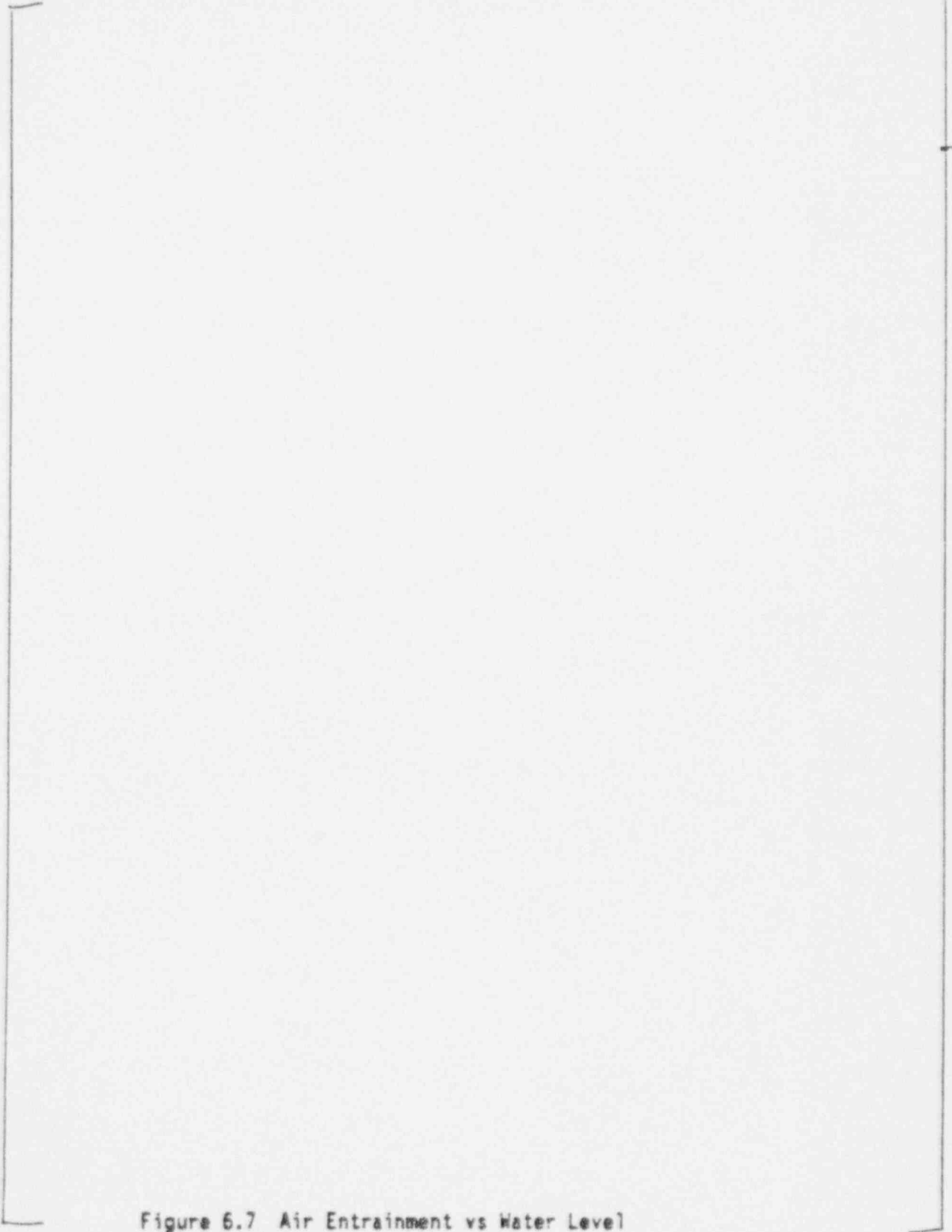


Figure 6.7 Air Entrainment vs Water Level  
(3" ID Step Nozzle by 12" Length at Bottom of Simulated H.L.)



a, b

Figure 6.8 Vortexing Water Level vs. Froude No.  
( $\phi$  3.86" Intermediate Pipe x 12" Length)

a, b

Figure 6.9 Comparison of Test Results  
( $\phi$  3.86" Intermediate Pipe x 12" Length)

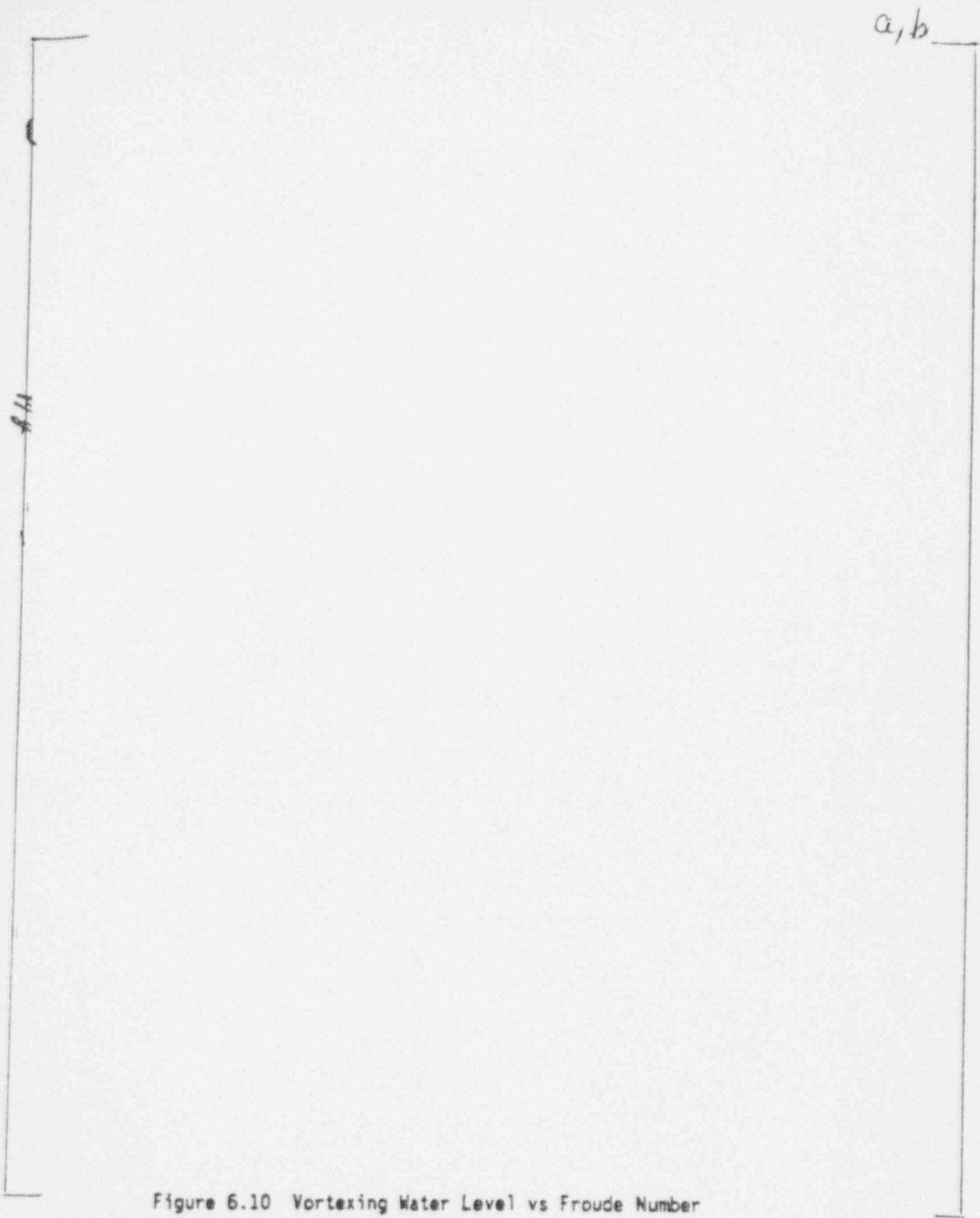


Figure 6.10 Vortexing Water Level vs Froude Number  
( $\phi$  3.86" ID Intermediate Pipe x 5.56" Length)

a, b

Figure 6.11 Comparison of Test Results  
( $\phi$  3.86" Step Nozzle x 5.56" Length)

a, b

Figure 6.12 Vortexing Water Level vs. Froude Number  
( $\phi$  3.86" ID Intermediate Pipe x 4.3" Length)

a, b

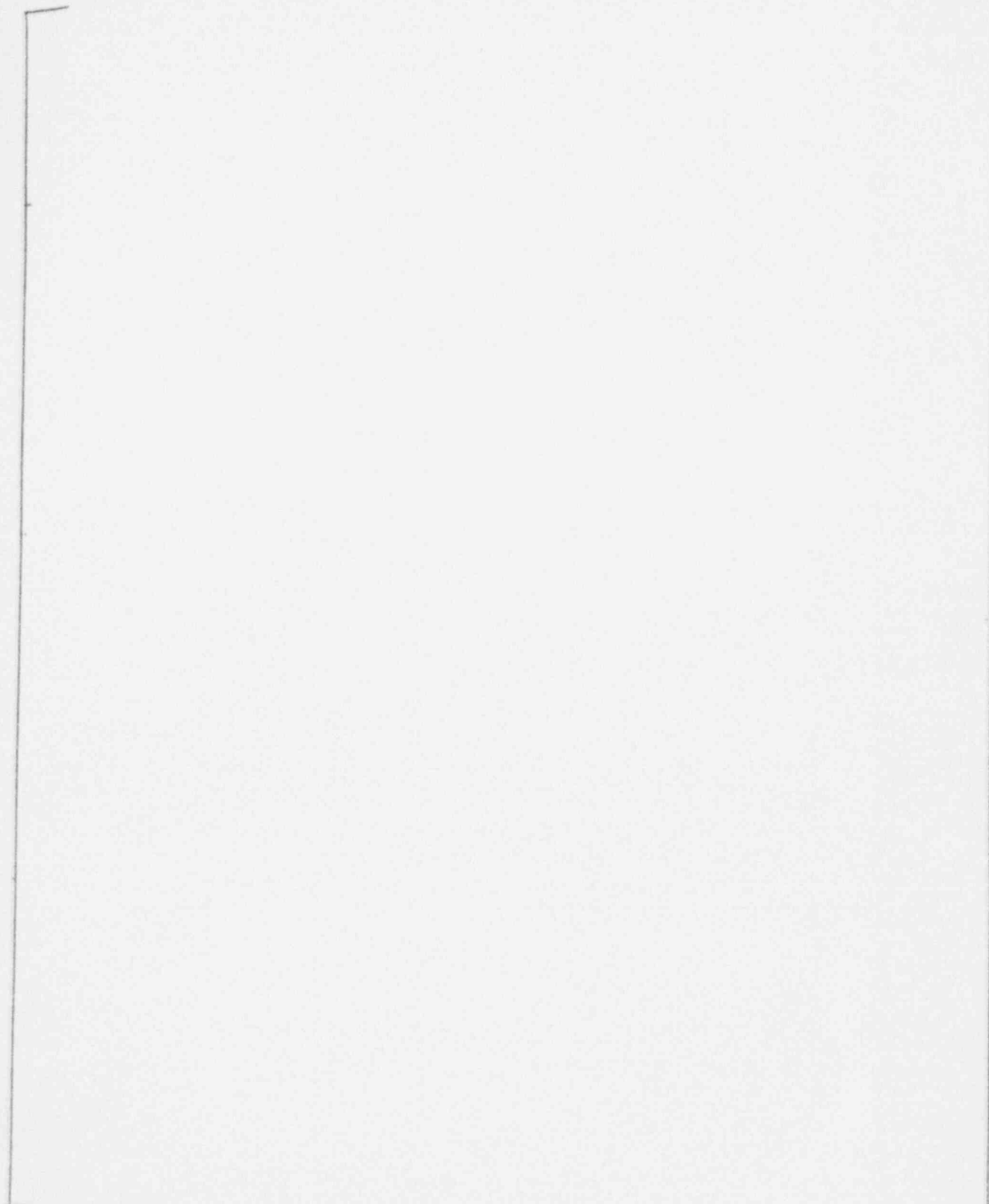


Figure 6.13 Comparison of Test Results  
( $\phi$  3.86" Step Nozzle x 4.3" Length)

a, b

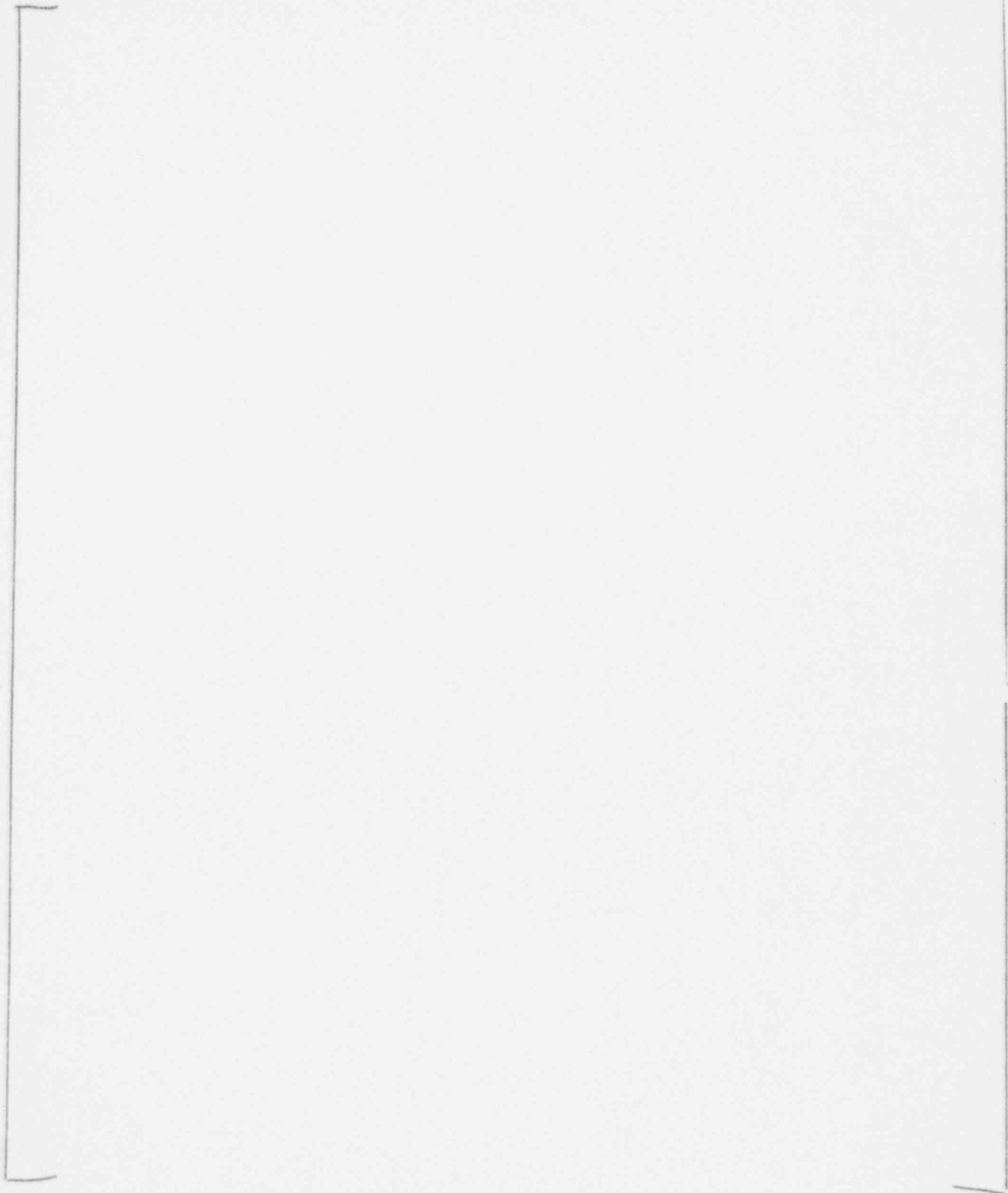


Figure 6.14 Comparison of Test Results  
(e 3.86" Step Nozzle x 2.876" Length)

a, b

Figure 6.15 Comparison with MHI Test  
(RHR Nozzle Located at Bottom of Hot Leg Case)



a, b

Figure 6.16 Vortexing Water Level vs Froude Number  
Simulated RHR Pipe at 45° (WOG's Test)

a, b

Figure 6.17 Comparison of Data with Different Simulated RHR Pipe  
(Simulated RHR Pipe is Connected to Bottom of H.L.)

## 7.0 BIBLIOGRAPHY

- (1) A. K. Jain; K. G. R. Raju; R. J. Garde; "Air Entrainment In Radial Flow Towards Intakes." Journal Of The Hydraulics Division, Sept. 1978.
- (2) A. K. Jain; K. G. R. Raju; R. J. Garde; "Vortex Formation At Vertical Pipe Intakes." Journal of The Hydraulics Division, Oct. 1978.
- (3) Harleman, D.R.F.; Morgan, R.L. and Purple, R.A.; "Selective Withdrawal From A Vertically Stratified Fluid." Proceedings, Eighth Congress of The International Associations for Hydraulic Research 1959, Paper 10-C
- (4) L.K. Lau; "Loss of Decay Heat Removal System Caused By Vortexing In Current PWR Plants and Its Applicability to AP 600." Westinghouse Report NPD-FS-0035, October 16 1987.
- (5) Mitsubishi Heavy Industry's Laboratory Report "Study On Air Pull-Through (Suction) In RHRP Suction Line." June 1987
- (6) Westinghouse Report WCAP 11916; "Loss Of RHRS Cooling While The RCS Is Partially Filled." September 1988.

8.0 APPENDIX

Appendix A - Calculation

Appendix B - Void Meter Calibration Program



APPENDIX A

SAMPLE CALCULATIONS

A-1.0 TEST MODELING CALCULATIONS

AP600 hot leg ID = 31" }

Test Model hot leg ID = 7" }

∴ linear scale  $\frac{7}{31} = 0.226$

(1) Froude Number Modeling, Fr

Model criteria: (Fr) plant = (Fr) model

$$Fr = \frac{V}{(gd)^{0.5}}$$

$$V = \frac{Q}{A} = \frac{Q}{\frac{\pi}{4} d^2} = \frac{4Q}{\pi d^2}$$

$$Fr = \frac{V}{(gd)^{0.5}} = \frac{4Q}{\pi d^2 \cdot g^{0.5} d^{0.5}}$$

$$Fr = \frac{V}{(gd)^{0.5}} = \frac{4Q}{\pi d^2 \cdot g^{0.5} d^{2.5}}$$

V = intake flow velocity  
d = intake ID  
g = gravitational acceleration  
Q = flow rate  
A = intake flow area

(2) Test Model Flow Rate Estimate,  $Q_{\text{Model}}$

$$\therefore (Fr)_{\text{model}} = (Fr)_{\text{plant}}$$

$$\left( \frac{40}{\pi g^{0.5} d^{2.5}} \right)_{\text{model}} = \left( \frac{40}{\pi g^{0.5} d^{2.5}} \right)_{\text{plant}}$$

or

$$\frac{Q_{\text{model}}}{(d_{\text{model}})^{2.5}} = \frac{Q_{\text{plant}}}{(d_{\text{plant}})^{2.5}}$$

$$\therefore Q_{\text{model}} = \left( \frac{d_{\text{model}}}{d_{\text{plant}}} \right)^{2.5} Q_{\text{plant}}$$

$$\frac{d_{\text{model}}}{d_{\text{plant}}} = \text{linear scale} = 0.226$$

$$Q_{\text{model}} = (0.226)^{2.5} Q_{\text{plant}}$$

$$Q_{\text{model}} = 0.0243 Q_{\text{plant}}$$

AP600 $Q_{\text{plant}}$	4403 gpm	3498 gpm	3004 gpm	2016 gpm	1193 gpm	617 gpm
Test Model $Q_{\text{model}}$	107 gpm	85 gpm	73 gpm	49 gpm	29 gpm	15 gpm

(3) Test Model Intake Flow Velocity Estimate,  $V_{\text{model}}$

Equating  $(Fr)_{\text{model}} = (Fr)_{\text{plant}}$  again

$$\left( \frac{V}{g^{0.5} d^{0.5}} \right)_{\text{model}} = \left( \frac{V}{g^{0.5} d^{0.5}} \right)_{\text{plant}}$$

or

$$V_{\text{model}} = \left( \frac{d_{\text{model}}}{d_{\text{plant}}} \right)^{0.5} V_{\text{plant}}$$

$$V_{\text{model}} = (0.226)^{0.5} V_{\text{plant}}$$

$$V_{\text{model}} = (0.475)(V_{\text{plant}})$$



A-2.0 TEST DATA REDUCTION AND CALCULATIONS

(1) Simulated RHR (2.0"ID) at Bottom of Simulated Hot Leg

(i) Froude no Estimate

$$Fr = \frac{4 Q_{model}^{0.5}}{\pi g^{0.5} d_{model}^{2.5}} = \frac{4 (Q_{model} \frac{gal}{min})^{0.5}}{(\pi) (32.2 \frac{ft}{sec^2})^{0.5} (d_{model} \text{ in})^{2.5}}$$

$$Fr = \frac{4 Q_{model} \frac{gal}{min} \cdot \frac{1 \text{ min}}{60 \text{ sec}} \cdot \frac{ft^3}{7.481 \text{ gal}}}{(\pi) (32.2)^{0.5} \frac{ft^{0.5}}{sec} \cdot d_{model}^{2.5} (\text{in} \cdot \frac{ft}{12 \text{ in}})^{2.5}} \frac{ft^2}{sec} \quad \checkmark$$

$$F_r = \frac{(0.2494) (Q_{model})}{(d_{model})^{2.5}}$$

where  $Q_{model}$  = test model flow rate, gpm

$d_{model}$  = test model intake ID, in

Ex.  $Q_{model}$  = 49 gpm and RHR pipe ID = 2.0" (no step nozzle case)

$$F_r = \frac{0.2494 (49)}{(2.0)^{2.5}} = 2.16$$

$Q_{model}$	10 gpm	49 gpm	73 gpm	107 gpm
Corresponding $Q_{plant}$	411 gpm	2016 gpm	3004 gpm	4403 gpm
Froude No.	0.44	2.16	3.22	4.72

(ii) Weber Number Estimate,  $W_e$

$$W_e = \frac{\rho V^2 d}{\sigma}$$

$\rho$  = fluid density

$\sigma$  = surface tension

$V$  = flow intake velocity

At room temperature and atmospheric pressure

$$\rho \approx 62.4 \frac{\text{lbm}}{\text{ft}^3}$$

$$\sigma \approx 0.005 \frac{\text{lb}_f}{\text{ft}}$$

$$d = 2 \text{ in.} = \frac{2}{12} \text{ ft}$$

$$\text{At } 49 \text{ gpm, } V = \frac{Q}{A} = \frac{(49 \frac{\text{gal}}{\text{min}}) (\frac{1 \text{ min}}{60 \text{ sec}}) (\frac{1 \text{ ft}^3}{7.481 \text{ gal}})}{\frac{\pi}{4} (\frac{2}{12})^2 \text{ ft}^2} = 5 \frac{\text{ft}}{\text{sec}}$$

$$W_e = \frac{(62.4) (5)^2 (\frac{2}{12}) (\frac{\text{lbm}}{\text{ft}^3}) (\frac{\text{ft}^2}{\text{sec}^2}) (\text{ft})}{(0.005 \frac{\text{lb}_f}{\text{ft}}) (32.2 \frac{\text{ft lbm}}{\text{lb}_f \cdot \text{sec}^2})}$$

$$W_e = 1614.91$$

$Q_{\text{model}}$	10 gpm	15 gpm	49 gpm	73 gpm	61 gpm	107 gpm	13.35 gpm
$V_{\text{model}}$	1.02 $\frac{\text{ft}}{\text{sec}}$	1.53 $\frac{\text{ft}}{\text{sec}}$	5 $\frac{\text{ft}}{\text{sec}}$	7.456 $\frac{\text{ft}}{\text{sec}}$	6.23 $\frac{\text{ft}}{\text{sec}}$	10.98	1.363
$W_e$	67.2	151.2	1614.9	3591	2507	7788	120

(2) Step Nozzle    <sup>a,b</sup> at Bottom of Simulated Hot Leg

(i) Froude No Estimate

$$Fr = (0.2494) \left( \frac{Q_{\text{model}}}{d_{\text{model}}} \right)^{2.5}$$

where  $Q_{\text{model}}$  = test model flow rate, gpm

$d_{\text{model}}$  = test model intake ID (step nozzle ID), in

Ex.  $Q_{\text{model}} = 49$  gpm and  $d_{\text{model}} =$     <sup>a,b</sup>

$$Fr = \frac{(0.2494)(49)}{\text{   <sup>a,b</sup>}}^{2.5}$$

$$Fr = \text{   <sup>a,b</sup>}}$$

<sup>a,b</sup>

(ii) Weber Number Estimate,  $W_e$

$$W_e = \frac{\rho V^2 d}{\sigma}$$

$$\rho = 62.4 \frac{\text{lbm}}{\text{ft}^3}$$

$$\sigma = 0.005 \frac{\text{lb}_f}{\text{ft}}$$

$$d = \left[ \frac{\quad}{12} \right]^{a,b} \text{ft}$$

$$\text{At} \left[ \frac{\quad}{\text{gpm}} \right]^{a,b} \left( 0.1092 \frac{\text{ft}^3}{\text{sec}} \right)$$

$$v = \frac{Q}{A} = \left[ \quad \right]^{a,b}$$

$$w_e = \left[ \quad \right]^{a,b}$$

$$\left[ \quad \right]^{a,b}$$

$$\left[ \quad \right]^{a,b}$$

$$w_e = \frac{\rho V^2}{g d} \geq 120$$

$$F_r = \frac{V}{\sqrt{g d}}$$

First series of tests conclude that a low Froude numbers results in a low critical vortexing water level. Therefore, it is desirable to keep the Froude member as low as possible. The test results (first series) also suggest that the Froude number can be as low as approximately 0.4 and the surface tension is still negligible.

∴ Set  $Fr = 0.4$

or  $\frac{V}{(gd)^{0.5}} = 0.4 \rightarrow \sqrt{d} = \frac{V}{(\sqrt{g})(0.4)} \rightarrow d = \frac{V^2}{(g)(0.4)^2}$

Since,  $Q_{\text{model}} = [ \quad ]^{a,b}$

$V = \frac{Q}{A} = \frac{Q}{(\frac{\pi}{4})(d^2)} = \frac{4Q}{\pi d^2} = [ \quad ]^{a,b} \frac{\text{ft}}{\text{sec}}$

$\therefore d = [ \quad ]^{a,b} (\text{ft})$

$d^5 = [ \quad ]^{a,b}$

$W_e = [ \quad ]^{a,b}$

Use standard size  $[ \quad ]^{a,b}$  for step nozzle.

APPENDIX B

VOID FRACTION METER  
DESCRIPTION/CALIBRATION

## B-1.0 INTRODUCTION

The objective of the current test program was to evaluate the effect of various geometric designs of the cold leg/RHR line junction on the entrainment of air in the RHR flow during operation of the RHR system with the coolant level at or near mid-loop. The design judged to be optimal, that is, resulting in minimum ingestion of air, will be recommended for inclusion into the AP-600 design.

The accurate measurement of entrained air, or void, in the simulated RHR line flow was required to accomplish the test objective. Direct measurements of local void fraction were made in the hot leg/RHR line simulation using a void meter manufactured by Auburn International. The meter actually measured the liquid fraction in the flow channel; the void fraction was taken as the complement of the liquid fraction.

The cylindrical cross-section of the RHR line simulation suggested the use of a Model 1081 void meter. This meter utilized four electrodes, connected in pairs that faced each other across a flow channel, with a rotating two-phase electrical current applied to the electrodes. A schematic planar layout of the Model 1081 void fraction probes as installed in the RHR line simulation used in the test program is shown in Figure B-1.

The liquid fraction at the location of the probes is determined by taking the ratio of the electrical resistance across the flow channel being monitored to the electrical resistance across a reference set of electrodes maintained in a solution with no voids. Typically, the meter is calibrated prior to testing by means of setting two points on the calibration curve. The two points used are void meter readings with the flow channel empty (totally voided or  $\alpha = 1.0$ ) and with the flow channel filled with the working fluid (no voids or  $\alpha = 0.0$ ).

The response of the meter to voids between the two limits may not linear. Thus, an in-situ calibration was performed to develop the appropriate correlation for actual void fraction versus measured void fraction between the channel empty-channel full end points.

This Appendix describes the in-situ calibration tests performed to support the use of the Model 1081 Auburn International void meter in the current test program.

## B-2.0 TEST OBJECTIVES

The objectives of the calibration tests performed with the prototypic RHR line simulation model hardware and the Auburn International void meter were:

- o Determine the performance of the Model 1081 void meter between calibration extremes ( $\alpha = 0.0$  and  $\alpha = 1.0$ ) for the RHR line simulation tested.
- o Develop the appropriate data base to develop a calibration for actual versus measured void fraction where the meter performance is not linear.
- o Define the sensitivity of the void meter readings to the positioning of void simulations within the flow channel bounded by the inside diameter of the RHR line simulation; evaluate uncertainty in measured void due to position of void in flow channel, if warranted.

By accomplishing the preceding objectives, the capabilities and limitations of the Auburn International void meters and associated probes as installed and used in the cold leg/RHR line simulation used in the current test program was determined.

## B-3.0 TEST DESCRIPTION

As described in Section B-4.1, the test model was constructed from sections of plastic pipe that were bolted together to form the desired hot leg/RHR line junction simulation. The void meter probes were located in a vertical run of the RHR simulation line below the hot leg/RHR line junction simulation. This cross section of the void meter installation is shown in the schematic diagram of Figure B-2.



A schematic diagram of the hardware arrangement employed for the calibration tests is also given in Figure B-3. The instrumented section of tubing was filled with water from a holding tank. The holding tank also served to provide a reference measurement of liquid conductivity. The instrument channels connected to both the reference probes and the RHR line simulation were calibrated prior to testing by setting the zero and full-scale readings with the flow channels between the probes empty and full, respectively, per manufacturer's procedure.

In general, the test procedure consisted of the following steps;

- o Fill the test section with water from the holding tank to the bottom of the top flange of the RHR line simulation.
- o Insert a simulated void from the top of the model section downward to the bottom plate elevation.
- o Record void meter reading directly from the digital volt meter (DVM) display.
- o Remove the void simulation, and refill the test section with water from the holding tank, if required, such that the void meter probes are covered with water.

The preceding steps were repeated for each void simulation tested.

#### B-4.0 Calibration Data

The data collected from the calibration testing is presented in the following sections.

##### B-4.1 Response to Known Cylindrical Voids

Eleven void simulations of differing sizes were used to define the performance of the Model 1081 void meter and its associated electrodes as installed in the hot leg/RHR line simulations tested. The void simulations were cylindrical

rods made of plexiglass, a non-conductive material. Each void simulation was inserted into the scaled RHR line such that the centers of the model cross section and the void simulation cross section coincided, resulting in a uniformly thick water-filled annular space between the RHR line and void simulations, the output of the void meter was recorded, and the void simulation was then withdrawn from the model. This process was repeated three times for each of the eleven void simulations used. The dimensions of the void simulation used, the calculated void fraction for the void simulation, and the corresponding three outputs for the Model 1081 void meter for each void simulation tested are listed in Tables B-1 for the 2.25 inch ID RHR line simulation used in the current test program.

From the data of Table B-1, it is noted that the largest void simulation used in the calibration tests resulted in a calculated void fraction of 44.6 percent. Of particular interest in the actual test program were the measurement of void fractions less than about 10 percent. Thus, the calibration test data provided for the accurate definition of void meter response over the range of operation of interest in the test program.

#### B-4.2 Regions of Sensitivity

The sensitivity of the Model 1081 void meter as utilized in the scale hot leg/RHR line model to a known void simulation was defined by positioning a cylindrical void simulation of known diameter at discrete locations within the instrumented RHR line section and recording the resulting void meter readings. Two different sizes of cylindrical void simulations were used for this series of calibration tests. As was the case with the calibration test described in Section 4.1, the void simulations were lengths of plexiglass rods. The positioning of the void simulations is shown in Figure B-3. The sizes of the void simulations and the data from the tests are given in Table B-2 for the 2.25 inch ID RHR line simulation used in the current test program.

## B-5.0 Discussion

A brief discussion of the calibration data presented in the preceding section follows.

### B-5.1 Non-Linearity of Response

The data of Table B-1 are plotted in Figure B-4: Note that, however, the measured liquid fractions are expressed as void fraction. The plot includes that the Model 1081 void meter as utilized in the scale model RHR line simulation generally does provide a linear response to increasing void fraction over the range of void simulations tested. Over the range of void fractions of  $0.0 \leq \alpha \leq 0.45$ , the calibration data could be reasonably approximated by the following linear equations.

$$\alpha_{Act} = 1.35 (\alpha_{Meas}) \quad (B-1)$$

where

$\alpha_{Act}$  = the actual void fraction in the flow channel

$\alpha_{Meas}$  = the void fraction in the flow channel as measured by the Model 1081 void meter.

The preceding equations was found to be a good fit to the calibration data for the RHR line simulation over the void fraction range of  $0.0 \leq \alpha_{Meas} \leq 0.45$ .

### B-5.2 Regions of Sensitivity

The data of Tables B-2 show that, for the void meter/probe design used in the test program, the indicated liquid fraction is somewhat sensitive to the static positioning of a void simulation in the field of measurement. During the actual testing, it was observed that the ingested void either tended to

form a vapor core or, due to the high level of mixing induced by the flow passing through elbows upstream of the void meter probes, the voids tended to be homogeneously distributed throughout the flow. In either case, the voids ingested by the flow do not maintain a static position as they pass through the void meter probes. Therefore, it was concluded that the observed sensitivity of measured void fraction to positioning of a void simulation in the measurement field was not applicable to the dynamic flow process obtain during testing. Rather, the calibration data of Table B-1, judged to be applicable for reduction of the test data.

#### B-6.0 Summary

Calibration tests were performed for the Model 1081 void meter/probe design combination using prototypic scale model hot leg/RHR line test hardware. The calibration test established the response of the void meter/probe design combination for the RHR line simulation tested. The sensitivity of the void meter probe response to the static positioning of a void simulation in the flow field was also established, but was subsequently determined to be not applicable to the experimental data due to the dynamic characteristics of the vapor and liquid flow as they passed through the void meter probes.

Table B-1  
 Hot Leg/RHR Line Vortex Generation Test  
 Response of Model 1081 Void Meter  
 to  
 Cylindrical Void Simulations  
 RHR Line Simulation Id = 2.25 Inches

Simulated Void Diameter (Inches)	Calculated Void Fraction $\alpha_{calc}$	Measured Liquid Fraction - $(1 - \alpha)_{Meas}$		
		Trial Number		
		1	2	3
0.194	0.007	0.995	0.994	0.996
0.251	0.012	0.992	0.991	0.991
0.375	0.028	0.975	0.979	0.982
0.433	0.037	0.971	0.972	0.970
0.502	0.050	0.964	0.961	0.965
0.562	0.062	0.957	0.951	0.954
0.755	0.112	0.914	0.912	0.915
0.868	0.149	0.888	0.876	0.886
1.050	0.218	0.824	0.824	0.828
1.120	0.248	0.799	0.795	0.800
1.503	0.446	0.638	0.638	0.643

Table B-2  
 Hot Leg/RHR Line Vortex Generation Test  
 Sensitivity of Model 1081 Void Meter/Probe Design  
 to  
 Void Location  
 RHR Line Simulation ID = 2.25 Inches

Simulated Void Diameter (Inches)	Calculated Void Fraction $\alpha_{calc}$	Measured Liquid Fraction - $(1 - \alpha)_{Meas}$								
		Void Position Number								
		1	2	3	4	5	6	7	8	9
0.375	0.028	0.974	0.982	0.990	0.983	0.976	0.982	0.989	0.981	0.978
0.502	0.050	0.960	0.968	0.982	0.969	0.961	0.969	0.977	0.968	0.965

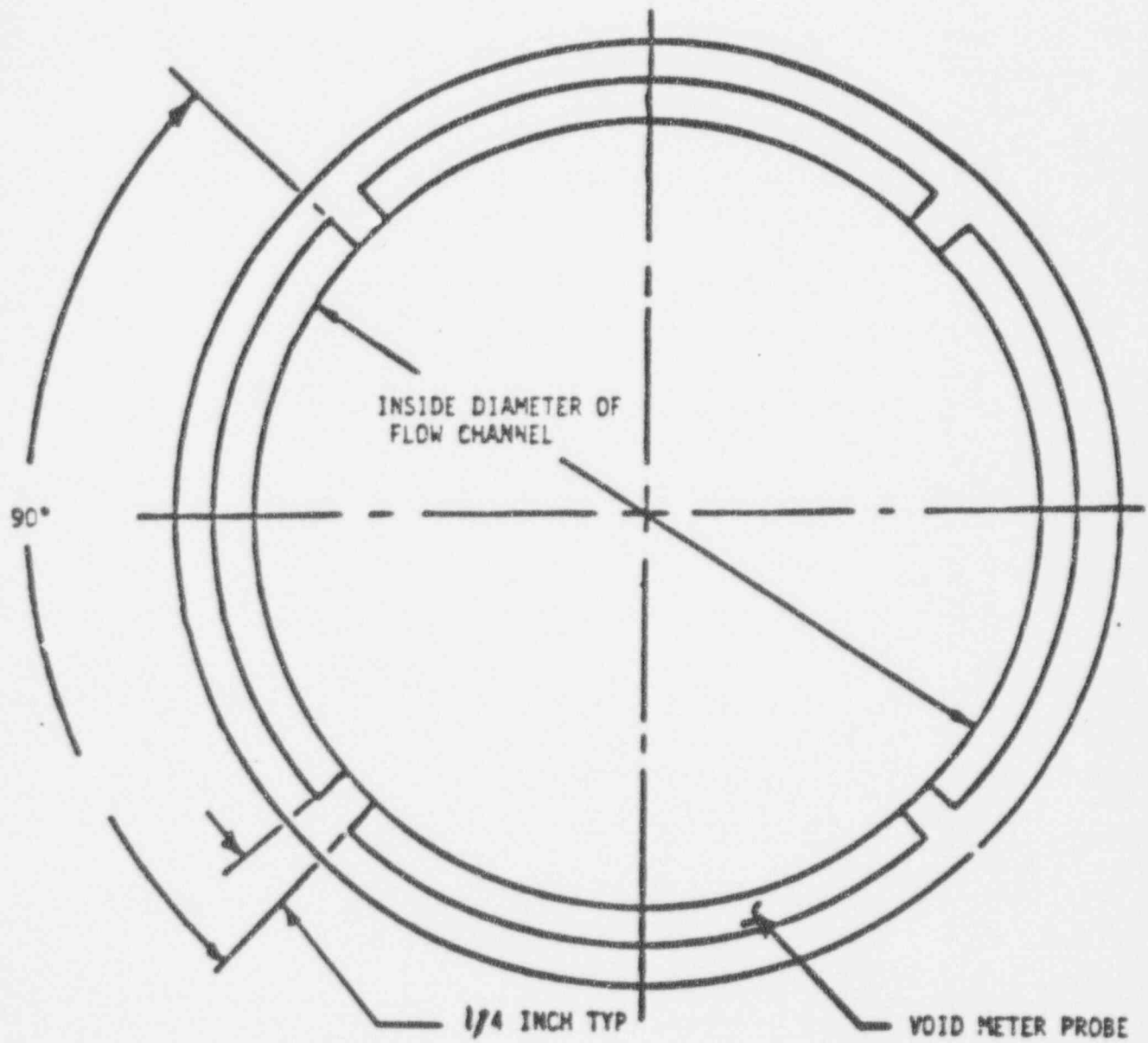


Figure B-1 Schematic of Typical Auburn  
Void Probe Installation

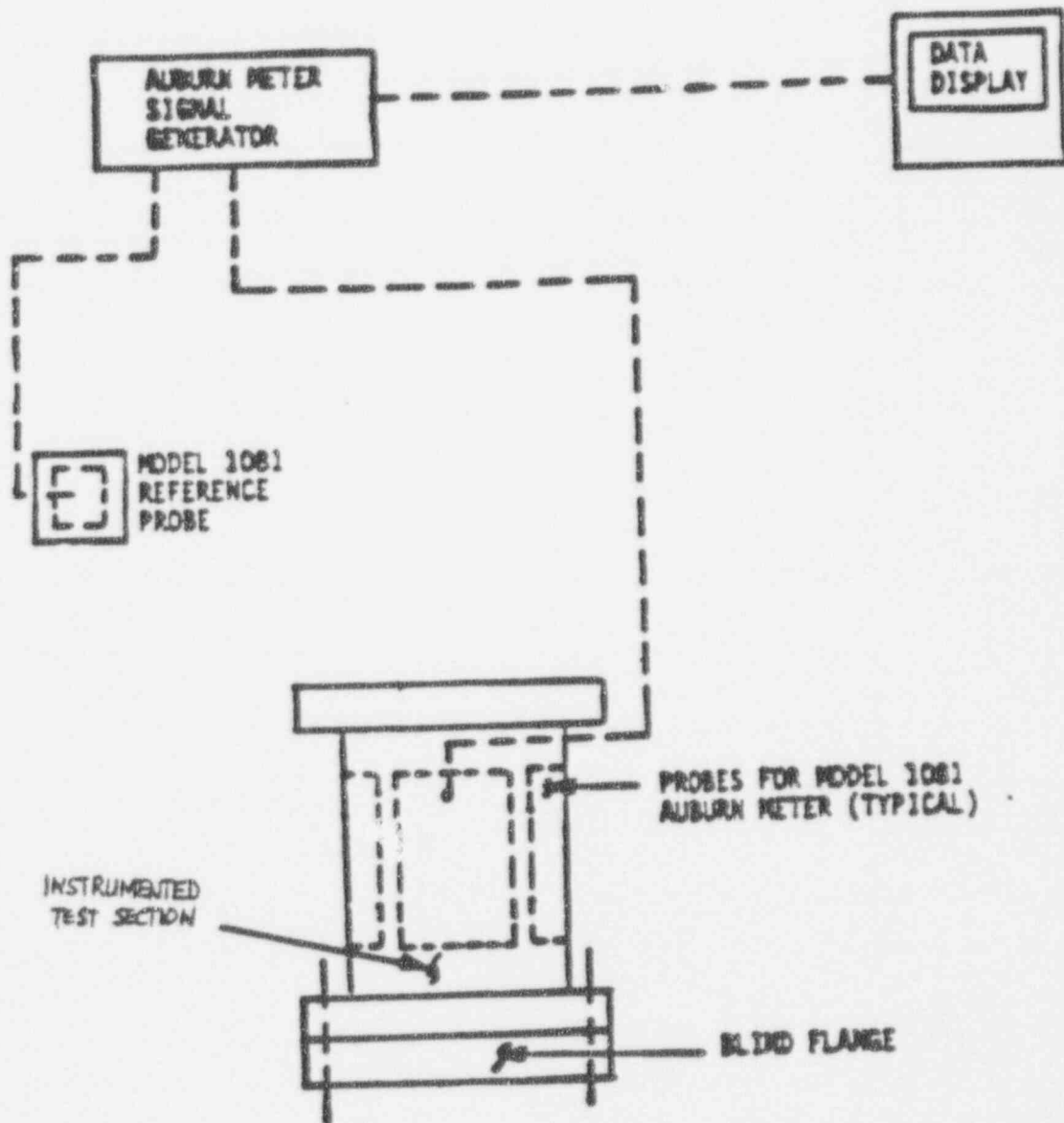


Figure B-2 Schematic of Auburn Void Meter Electrical Hook-up for Calibration Testing



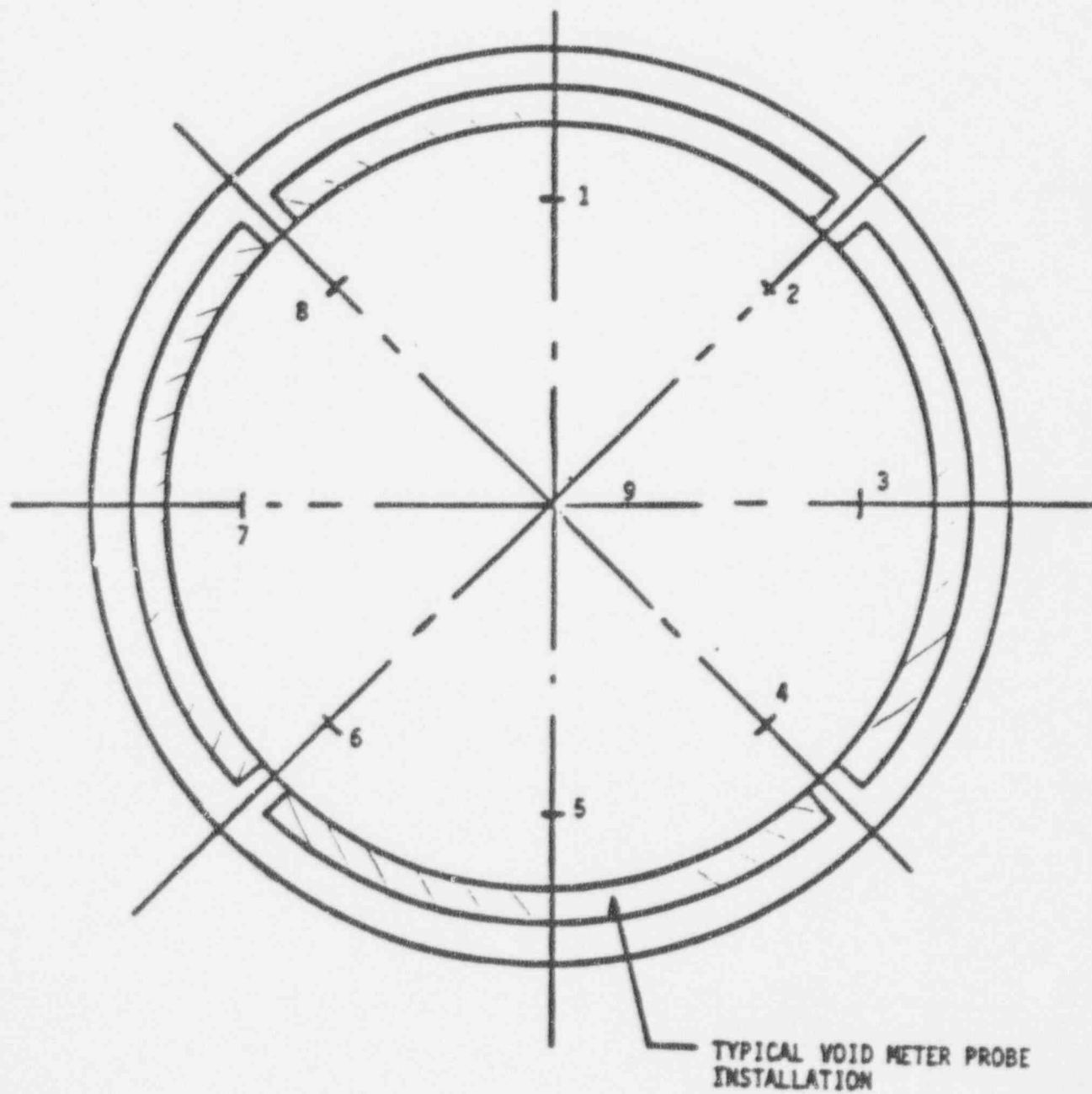


Figure B-3 Schematic of Void Simulation Locations  
Void Meter Sensitivity Tests